# MASTER THESIS

Department of Petroleum Production and Processing,
Mining University of Leoben.

By:

Stephan Reitler BSc

Under the supervision of:

Ao. Univ.-Prof. Dipl.-Ing. Dr. techn. Wilhelm Brandstätter

Leoben, December 2009

Reservoir simulation based on OpenSource software OpenFOAM

I declare in lieu of oath, that I wrote this Thesis and performed the associated research myself using only literature cited in this volume.

_____

Stephan Reitler

This Master Thesis is dedicated to my whole family. All my success is linked to their support and faith in me.

Acknowledgements

Table of Contents

List of Figures

List of Tables

Abstract

The purpose of reservoir simulation is to predict the future performance of a hydrocarbon bearing reservoir and find ways and means to optimize the recovery of the field. In the last two decades reservoir simulation has become more and more essential for the worldwide up-stream industry and numerous reservoir simulation tools have been launched on the market. These user-friendly, commercial software packages were designed to satisfy the needs of the petroleum industry for reliable production forecasts and reservoir characterizations.

When compared to commercial software, reservoir simulation based on OpenSource software OpenFOAM [12] would offer several advantages, particularly for academic reservoir simulation-training. For the first time, users have the possibility to gain direct access and to modify the source code. Apart from this benefit, OpenFOAM is equipped with integrated state of the art computational fluid dynamics (CFD) models [19]. OpenFOAM is also cost-efficient as it is freely available. However, OpenFOAM's user-friendliness is restricted by the fact that users are required to possess solid programming and specific mathematical skills, which are not required when using commercial software.

For this thesis an OpenFOAM based reservoir simulation solver called PRSFoam was developed and tested. The results of this OpenSource solver were compared to the performance of the commercial solver ECLIPSE [22] by Schlumberger [32]. Both tools were used to solve the single-phase black-oil model [4] for three test-reservoirs. The final conclusions of this thesis indicate that the results of both simulation tools only differ slightly in respect of achieved pressure performance and production rate. Consequently OpenFOAM reservoir simulation truly represents an expandable, useful and alternative option to costly commercial simulation tools.

Kurzfassung

Die Aufgabe von Lagerstättensimulatoren ist es, die zukünftige Ausbeute aus Kohlen-Wasserstoff Lagerstätten zu prognostizieren und dabei Wege und Mittel aufzuzeigen um die Feldausbeute zu optimieren. In den letzten zwei Jahrzenten nahm die Nachfrage nach verlässlichen Simulationsprogrammen in der Erdölindustrie weiter zu und zahlreiche Simulation-Tools wurden auf den Markt gebracht. Diese benutzerfreundliche, kommerzielle Software wurde alleine zu dem Zweck entwickelt, die Nachfrage der Erdölindustrie nach möglichst verlässlichen Produktionsprognosen und entsprechender Lagerstättencharakterisierung zu decken.

Bei dem Vergleich eines kommerziellen Lagerstättensimulators mit der OpenSource Software OpenFOAM sind gewisse Vorteile der Letzeren zu erkennen, welche besonders für den universitären Bereich eine interessante Rolle spielen könnten. OpenFOAM erlaubt erstmals den direkten Zugriff auf den Source-Code des Programmes und ermöglicht es somit dem Benutzer spezifische Probleme mit Hilfe von modernen CFD Modellen zu lösen. Ein weiterer Vorteil von OpenFOAM wäre eine Reduzierung der Lizenzkosten, da OpenFOAM frei und unentgeltlich verfügbar ist. Doch auch bei OpenFOAM gibt es Einschränkungen der Benutzerfreundlichkeit. Der Nutzer muss schon ein gewisses Maß an programmiertechnischem und mathematischem Grundwissen vorweisen können, das bei einer kommerziellen Lagerstättensoftware nicht zwangsläufig notwendig ist.

Um die Integrität von OpenFOAM als Lagerstätten Simulations-Software zu ermitteln wurde ein Solver namens PRSFoam entwickelt und getestet. In dieser Arbeit löst PRSFoam die Druckgleichung für drei Testlagerstätten anhand eines ein-phasigen "black-oil" Modells. Die Ergebnisse wurden anhand der namhaften kommerziellen Lagerstätten-Tools ECLIPSE verglichen. Es lässt sich feststellen, dass die Ergebnisse der Testmodelle bei beiden Programmen nur gering in Bezug auf Druckverläufe und erzielten Produktionsraten voneinander abweichen. Hieraus lässt sich schließen, dass OpenFOAM unter bestimmten Voraussetzungen durchaus mit kommerziellen Simulationsprogrammen mithalten kann und repräsentiert – vor allem in der Hochschullehre – eine instruktive, nützliche und auch ausbaufähige Alternative zu kommerziellen Software.

1. Introduction

An increasing demand for energy combined with stagnating supplies will sooner or later confront mankind to an essential problem: the scarcity of hydrocarbons. Especially developed countries are particularly dependent on energy-supplies of countries rich in resources. The estimated capacity of mapped out hydrocarbon reserves predict a total depletion within the next 80 years. [4] As there presently is no quantitative and qualitative alternative within reach, it is an obvious need to enhance the recovery of existing and future hydrocarbon reservoirs. Computational reservoir models, based on seismic and geological data are developed to create long and short term forecasts. Production engineers follow up these plans to maximize reservoir production performance, to confirm corporate policy, fulfill economic targets and lastly enhance total field production.

Reservoir models are essential in order to understand and predict complex phase behavior in a reservoir through existing and planned wells. During the last decades, the demands for modern reservoir models, created by powerful simulators, increased rapidly. New features and enhancements ease the data gathering, data processing and visualization of hydrocarbon bearing reservoirs and finally the process of decision making. [4]

It is not a secret, that hydrocarbon recovery projects have the potential to be highly profitable for the contracting companies. On the other hand, these recovery projects, which require high capital investment, are risky as they are dependent on precarious development and production strategies. To minimize exposure, modern reservoir simulation is used to achieve the highest possible exploitation results and to study relevant production strategies. [4]

The growing acceptance of professional reservoir simulation in the petroleum industry during the last decades can further be attributed to the progress made in computing facilities. Various companies have introduced a number of high-quality simulation packages to pre-process, solve and post-process multi-phase flow in complex reservoirs. Most of these tools are able to switch between black-oil, compositional, chemical or thermal displacement models. [28] Common reservoir software tools can be classified into two categories:

- <u>Independent simulators</u> are introduced by oilfield-service-providers and up-stream related software designers. Well known examples are "REVEAL" [29] by Petroleum Experts Inc. and "ECLIPSE" [22] by SIS-Schlumberger.

- <u>In-house simulators</u> have been developed by several major oil and gas companies to grant independency from external service companies and ease company internal data manipulation and preparation. Examples are "POWERS" [30] by Saudi Aramco and "CHEARS" [31] by Chevron.

Since, the scope of reservoir software has increased to solve gigantic and complex multi-phase reservoirs, the complexity for usage increased at the same scale. Users have to undergo a great deal of time consuming training efforts before being able to simulate. Another crucial drawback of commercial reservoir simulation software is the license costs, which can amount to 35.000 Euros per year per desktop. [4]

Altogether, certain factors – be it the high license costs, the complex structure of modern reservoir simulators or the restriction in access to its source code – limit the efforts in the ongoing research. These disadvantages are obstacles, when commercial reservoir simulation software is to be used for academic purposes.

In 2005 the powerful OpenSource CFD software Open Field Operation and Manipulation, short OpenFOAM [15], was released. For the first time it is possible to remodel high-performance CFD software and obtain direct access to its source code: therefore it is self-evident to test the potential and abilities of reservoir simulation based on OpenSource software OpenFOAM.

Editing the source code provides a vast range of versatility and enables its users to create problem specific solvers and utilities in the future.

- OpenFOAM could be used to solve process-intensive turbulent flow around high-productive wells, using Navier-Stokes equations. This could be important to predict pressure loss and compare different kinds of production scenarios.

- Using OpenFOAM, there is no limitation of faces bounding each spatial discretized control volume. This "arbitrary unstructured mesh" offers greater freedom in mesh generation in particular when the geometry is complex. [17]

- The displacement process at the front: "liquid fingering" or effects of enhanced oil recovery methods, such as polymer flooding [38], in-situ combustion [38], steam flooding [38] and etc can be simulated.

However, OpenFOAM is not a panacea to solve complex reservoir problems in a minute. This OpenSource freedom requires a well-founded knowledge of the underlying methods, physics and programming techniques involved. Therefore, this work is intended to be an introduction and a guideline for reservoir engineers, which need OpenFOAM for simulating single-phase flow through porous media. The steps, the workflow and the integration of physical and mathematical models are covered for an OpenSource reservoir simulator.

To accomplish the task, two single-phase test-reservoirs and one single-phase injection-production scenario are created to compare results under equal production and boundary conditions. Results of these test cases and the conclusions will complete this work.

2. Basic Reservoir Simulation Models

A naturally occurring hydrocarbon reservoir is a three-dimensional, heterogeneous, anisotropic, porous rock domain, which can be saturated with a fluid of various components. All processes within this reservoir are associated to fluid flow and mass transfer.

Reservoir simulation aims to predict these fluid flows within the reservoir to finally compute possible forecasts and is thereby used to find ways to optimize the recovery of hydrocarbons under various operating conditions. It involves four interrelated stages, which can be seen in Figure (2-1). [4]
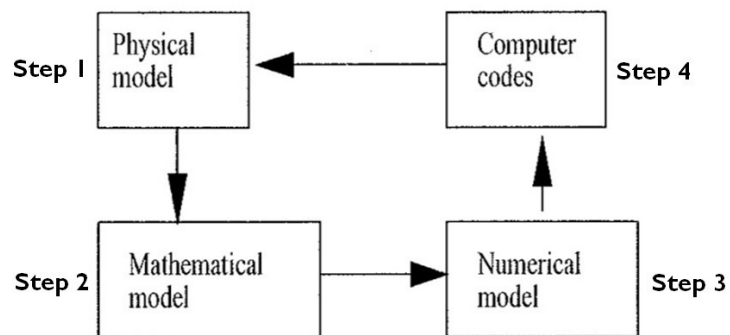
Figure 2-1: Major steps in reservoir simulation study [4]

- First of all, a physical model of relevant processes is set up, incorporating the necessary physics to describe all essential features of the underlying physical phenomena.

- Second, a set of coupled systems of time-dependent nonlinear partial differential equations is developed and analyzed for existence, uniqueness, stability and regularity.

- Third, a numerical model with the basic properties of both the physical and the mathematical models are derived and analyzed.

- Fourth, computer algorithms and codes are developed to efficiently solve the systems of linear and nonlinear algebraic equations arising from the numerical discretization. Each stage represents an essential step in reservoir simulation. Additionally to these stages boundary conditions are necessary to structure the simulation and keep the numerical method confined. These conditions are related to factors, such as case geometry, operating conditions and environmental conditions. [4]

This chapter will focus on basic models and equations to characterize the physical phenomena of dynamic flow and mass transfer through a permeable hydrocarbon reservoir. It will start from a general definition of reservoir characteristics, such as rock properties (porosity, rock compressibility and permeability), fluid properties, simulation models (Darcy's law, equation of state, equation of continuity) and will finally end up in a simplified formulation for solving a black-oil reservoir problem. [4] [1]

2.1   Fundamental Properties of Porous Media

Reservoir properties of interest reflect the capacity of a rock to store and transmit the fluid in its pores. These relevant properties are: rock porosity, rock permeability and rock compressibility. [24]

Porosity is the fraction of a rock that is pore space. In detail, the porosity ϕ is defined as the ratio of pore volume to total volume, which can be expressed as:

$$\phi = \frac{V_p}{V_T} = \frac{V_T - V_S}{V_T} \qquad (2\text{-}1)$$

where V_p defines the empty pore volume, V_T represents the total volume and V_S defines the solid fraction within the total volume. [24] [4]

The term porosity includes interconnected and isolated pore space. Only interconnected, effective porosity is of crucial importance in reservoir engineering, as it is able to accumulate and also transmit hydrocarbons. If pores are less connected to the surrounding, hydrocarbons are trapped and unable to move. Porosity varies from 0,25 % for a poor consolidated block down to 0,1% for a high compacted reservoir rock. If the porosity also varies with the location within the reservoir, it is termed as heterogeneous porosity. [4]

Rock compressibility: The reservoir rock is not considered to be a rigid system. Variation of pore volume with pore pressure can be taken into account by the pressure dependence of porosity, which can be assumed to be constant in the majority of cases. [4] Since porosity represents a part of volume, the general compressibility equation for fluid mechanics can be used to describe the rock compressibility-factor c_R under isothermal conditions **T**. The rock compressibility-factor c_R is defined by: [4] [24]

$$c_R = \frac{1}{\phi}\left(\frac{d\phi}{dp}\right)_{\mathbf{T}} \qquad\qquad (2\text{-}2)$$

Permeability: describes the ability of a rock to conduct fluids, through its interconnected pores. A high permeability k is probably the most important attribute for a hydrocarbon reservoir, as permeability indicates connectivity and therefore the ability of phases to flow within the reservoir. Permeability often varies with location and even at the same location, may depend on flow direction. [24] [4]

Considering a permeable control volume, pressure and the resulting permeability can be measured and calculated in three directions using Darcy's law. Thus leading to a 3 by 3 tensor, which is realized using a 3 by 3 matrix being both symmetric and positive, as seen in equation (2-3): [4] [22]

$$\bar{k} = \begin{bmatrix} k_{11} & 0 & 0 \\ 0 & k_{22} & 0 \\ 0 & 0 & k_{33} \end{bmatrix} = \mathrm{diag}(k_{11}, k_{22}, k_{33}) \qquad\qquad (2\text{-}3)$$

Vertical permeability $k_V = k_{33}$ is usually different from horizontal permeability k_H, due to rock mechanism and overburden pressure. The horizontal permeability is generally larger

than the vertical permeability. If $k_{11} = k_{22} = k_{33}$, the porous media is called isotropic and is a scalar. [4]

Since permeability is the capacity of a rock to conduct fluid through its interconnected pores, the next chapter will introduce important models to describe single phase flow through permeable media.

2.2 Equations of Single-Phase Filtration

Describing the flow through a porous medium, one must distinguish between mass flow and filtration. During mass flow all mass particles of the system are moving. In the case of filtration only certain parts of the particles are moving, while all others form a solid matrix. [24] The following mathematics is included in the literature of Dr. Zoltan Heinemann [1] [3] [24] and Dr. Zhangxin Chen [4].

2.2.1 Darcy's Law of Fluid Flow

Darcy's Law describes the fluid flow through a porous medium at specific conditions. The law was formulated and published by Henry Darcy in 1856 and is based on the results of several water-flow experiments through beds of permeable sand. A schematic illustration of Darcy's experiment can be seen in Figure 2-2. [4] [24]
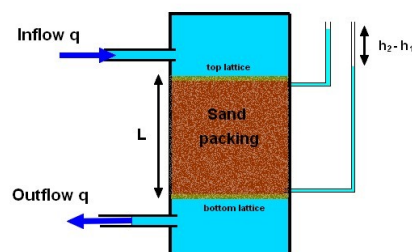
Figure 2-2: Darcy's experiment of flow through porous media [24]

A defined water rate (Inflow q = Outflow q) enters a closed test-vessel on top. The vessel is filled with water and a permeable sand packing; of the length L, the diameter A which exhibits the permeability k. The sand packing is placed in the center and therefore bounded by a fixed lattice to prevent solid movement. Water flows from the higher pressure potential at the top to the lower pressure potential at the bottom. This pressure difference Δp_V is enforced by gravitational force g. Hence, the difference in piezometric head (h$_2$ - h$_1$) can be used to calculate the corresponding pressure difference in equation (2-4): [24]

$$\Delta p_V = \rho g * (h_2 - h_1) \qquad (2\text{-}4)$$

This pressure difference Δp_V is valid for vertical flow.

The pressure differences Δp in natural reservoir projects are usually influenced by reservoir driving forces, such as compressibility of rock and phases, gas-cap drive, solution gas drive, water drive, buoyancy force and artificial precipitated driving forces.

A law to define the permeability of a porous medium was introduced at the World Oil Congress in the year 1933. Based on Darcy's experiments, this law describes the flow of a fluid (rate q, viscosity μ) through a porous medium (permeability k, the length L and the cross-sectional area A) causing a pressure difference of Δp (Figure 2-3) and was thenceforth known as Darcy's Law. [4]
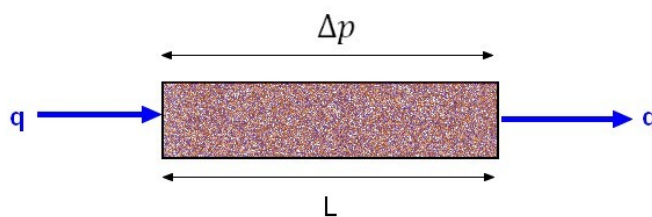
Figure 2-3: Volumetric flow rate [4]

Darcy's Law (2-5) is valid for a laminar and steady-state one-phase flow of an incompressible fluid. [24]

$$q = -\frac{A * k}{\mu} \frac{\Delta p}{L} \qquad (2\text{-}5)$$

Considering equation (2-5), the Darcy velocity $\mathbf{u}$ is calculated by $u = {}^{q}/_{A}$, which leads to:

$$u = -\frac{k}{\mu} \frac{\Delta p}{L} \qquad (2\text{-}6)$$

For a 3D flow system with the gravitational force g, the differential form of the Darcy velocity, also known as superficial velocity $\mathbf{u}$ is:

$$\mathbf{u} = -\frac{1}{\mu} \bar{k}(\nabla p - \rho g \nabla z) \qquad (2\text{-}7)$$

where $\bar{k}$ is the absolute permeability tensor (equation 2-3) of the heterogenic porous media, g is the magnitude of the gravitational acceleration, z is the depth and ∇ is the gradient operator, defined by:

$$\nabla p = \left(\frac{\partial p}{\partial x_1}, \frac{\partial p}{\partial x_2}, \frac{\partial p}{\partial x_3} \right) \qquad (2\text{-}8)$$

The x_3-coordinate in equation (2-8) has to be the vertical downward direction.

$(\nabla p - \rho g \nabla z)$ is also known as the pressure potential function Ψ.

$$\Psi = (\nabla p - \rho g \nabla z) \qquad (2\text{-}9)$$

Incompressible fluids: The pressure potential function of equation (2-9) includes the density of the fluid ρ. When the fluid is incompressible the density is assumed to be constant. [4] [24]

2.3   Equation of Continuity

The equation of continuity, also known as material balance equation, describes the conservation of mass within a continuum. For this purpose a control volume in a rectangular coordinate system, embedded into a porous medium is considered. It can be seen as a mathematical statement, which equates the rate at which mass enters a system is equal to the rate at which mass leaves the system. The flow through this porous system is described by Darcy's Law. [24]

To simplify the equation of mass change, only one symmetrical block is selected, whereby the faces are considered to be parallel to the Cartesian coordinate system. This selected block has the dimensions Δx_1, Δx_2, and Δx_3, and can be seen Figure 2-4. [4] [24]
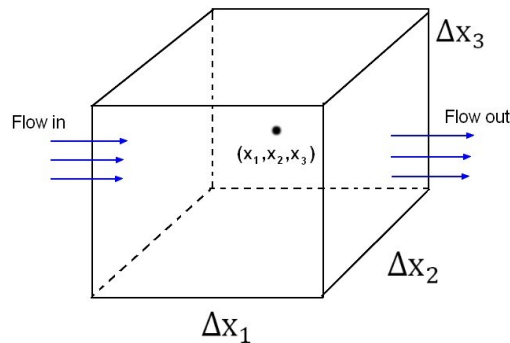
Figure 2-4: Flow through a differential volume [4]

The spatial and temporal notation will be represented by the variables $x = (x_1, x_2, x_3)$ and t. The superficial velocity (2-7) is given by $\mathbf{u} = (u_1, u_2, u_3)$. The x_i-component of the mass flux of the fluid is ρu_i, with units mass flow per area per time. [4] [20]

Referring to Figure 2-4, the mass inflow across the surface at $x_1 - \frac{\Delta x_1}{2}$ per unit time is:

$$(\rho u_1)_{x_1 - \frac{\Delta x_1}{2}, x_2, x_3} \Delta x_2 \, \Delta x_3 \qquad\qquad (2\text{-}10)$$

and the mass outflow at $x_1 + \frac{\Delta x_1}{2}$ is therefore:

$$(\rho u_1)_{x_1+\frac{\Delta x_1}{2}, x_2, x_3} \Delta x_2\, \Delta x_3$$

The mass inflow and outflow across the surfaces are similarly in $x_2 -$ and $x_3 -$ coordinate direction. For x_2 direction:

$$\text{inflow:} \quad (\rho u_2)_{x_1, x_2-\frac{\Delta x_2}{2}, x_3} \Delta x_1\, \Delta x_3 \quad \text{outflow:} \quad (\rho u_2)_{x_1, x_2+\frac{\Delta x_2}{2}, x_3} \Delta x_1\, \Delta x_3 \qquad \text{(2-11)}$$

And finally the mass inflow and outflow across the surfaces for x_3 coordinate direction:

$$\text{inflow:} \quad (\rho u_3)_{x_1, x_2, x_3-\frac{\Delta x_3}{2}} \Delta x_1\, \Delta x_2 \quad \text{outflow:} \quad (\rho u_3)_{x_1, x_2, x_3+\frac{\Delta x_3}{2}} \Delta x_1\, \Delta x_2 \qquad \text{(2-12)}$$

To meet requirements of a time dependent flow rate through the differential volume, a temporal quantity has to be introduced. With $\frac{\partial}{\partial t}$ being the time differentiation, mass accumulation due to compressibility per unit time leads to:

$$\frac{\partial(\rho\phi)}{\partial t} \Delta x_1 \Delta x_2 \Delta x_3 \qquad \text{(2-13)}$$

and the removal of mass from the cube, meaning the mass accumulation due to a sink of flow rate q, is:

$$-q\, \Delta x_1 \Delta x_2 \Delta x_3 \qquad \text{(2-14)}$$

Considering equations (2-10), (2-11), (2-12), (2-13) and (2-14), the difference between the mass inflow and outflow into all three directions is equal to the sum of mass accumulation within this volume:

$$\left[(\rho u_1)_{x_1 - \frac{\Delta x_1}{2},\, x_2,\, x_3} - (\rho u_1)_{x_1 + \frac{\Delta x_1}{2}\, x_2,\, x_3} \right] \Delta x_2 \Delta x_3 + \qquad (2\text{-}15)$$

$$+ \left[(\rho u_2)_{x_1,\, x_2 - \frac{\Delta x_2}{2},\, x_3} - (\rho u_2)_{x_1,\, x_2 + \frac{\Delta x_2}{2},\, x_3} \right] \Delta x_1 \Delta x_3 +$$

$$+ \left[(\rho u_3)_{x_1,\, x_2,\, x_3 - \frac{\Delta x_3}{2}} - (\rho u_3)_{x_1,\, x_2,\, x_3 + \frac{\Delta x_3}{2}} \right] \Delta x_1 \Delta x_2 =$$

$$= \left(\frac{\partial (\rho \phi)}{\partial t} - q \right) \Delta x_1 \Delta x_2 \Delta x_3$$

Dividing equation (2-15) by $\Delta x_1 \Delta x_2 \Delta x_3$, and letting $\Delta x_i \rightarrow 0$, i = 1, 2, 3, we obtain the so-called "mass conservation equation":

$$\frac{\partial}{\partial t}(\phi \rho) = -\nabla(\rho \mathbf{u}) + q \qquad (2\text{-}16)$$

whereby ∇ is the divergence operator:

$$\nabla \mathbf{u} = \frac{\partial u_1}{\partial x_1} + \frac{\partial u_2}{\partial x_2} + \frac{\partial u_3}{\partial x_3} \qquad (2\text{-}17)$$

It has to be considered, that the rate q in equation (2-16) is positive for outflow and negative for inflow.

The "mass conservation equation" (2-16) is the basis of various reservoir simulation models. These models cover just a specific type of reservoir problem to keep the incidental case preparation and processing time as short as possible. Well known types of simulation models are listed in Table 2-1. The OpenSource solver presented in this thesis (chapter 4.1.1) will solve a simplified black-oil reservoir problem.

Principal Types of Simulation Models		
Model	**Advantages**	**Disadvantages**
Black-Oil	- fast - robust - wide spread and reliable	- pressure dependent fluid properties - limited to primary production and waterfloods
Chemical	- account for chemical compound - polymer and surfactant flooding	- complex fluid property changes - numerical dispersion - reliability of modelling chemical reactions
Thermal	- account for temperature effects - steam cycling, steamflooding	- performance, instability - additional equations and calculations necessary
Compositional	- accurate fluid description - account for compositional effects - equation of state calculations	- performance, instability - numerical dispersion - high computing cost

Table 2-1: Overview of simulation models [28]

2.4 The Black-Oil Model

There exist various types of mathematical models to describe the flow through porous media (Table 2-1). Simulating a three phase-, three dimensional black-oil model was one of the first efforts in the early 60's. It is assumed, that next to water, the hydrocarbon phase can be divided into a gas- and an oil component, respectively in a stock tank at surface pressure and at standard temperature. There is a mass transfer between oil and gas phase during production, due to pressure drop, but there is no mass transfer between water and hydrocarbon phase. [3] [4]

The black-oil model can be described best as a set of partial differential equations, representing the saturation and pressure in a reservoir. [3]

The introduction of the black-oil model in chapters 2.4.1 and 2.4.2 is included in literature of Dr. Zhangxin Chen [4].

2.4.1 Basic Black-Oil Equations for Simultaneous Flow of Three Phases

From now on it is important to distinguish between phase and component.

- Phase refers to a chemically homogeneous region of fluid that is separated from another phase by its interface. For example the clear interface between oil and water.

- Component is a single chemical species that may be present in a phase. For example, the water-phase in a reservoir contains components of water, sodium chloride, dissolved oxygen and many more. [4]

Because of mass interchange between the oil and gas phases, mass is not conserved within each phase, but rather the total mass of each component must be conserved. To cover the water-phase, modified equation (2-16) for two-phase flow leads to:

for water:
$$\frac{\partial}{\partial t}(\phi \rho_w S_w) = -\nabla(\rho_w \mathbf{u}_w) + q_W \qquad (2\text{-}18)$$

where S_w stands for the saturation of the water-phase within the porous medium.

for oil:
$$\frac{\partial}{\partial t}(\phi \rho_{oo} S_o) = -\nabla(\rho_{oo} \mathbf{u}_o) + q_o \qquad (2\text{-}19)$$

Equation (2-19) covers component oil, where ρ_{oo} denotes the partial density of the component oil, whereby the first subscript defines the phases and the second subscript identifies the component. [4] In the case of ρ_{oo}, it is the partial density of component oil in the oil phase.

for gas
$$\frac{\partial}{\partial t}\big(\varphi(\rho_{go}S_o + \rho_g S_g)\big) = -\nabla(\rho_{go}\mathbf{u}_o + \rho_g \mathbf{u}_g) + q_g \tag{2-20}$$

Introducing Darcy's Law for superficial velocity (2-7) to solve the velocity for a number of α-phases:

$$\mathbf{u}_\alpha = -\frac{1}{\mu_\alpha}\bar{k}_\alpha(\nabla p_\alpha - \rho_\alpha g\nabla z) \tag{2-21}$$

whereby α is either water, oil or gas.

It is assumed, that all phases fill the void pore space, and expected that the total saturation is $S_w + S_o + S_g = 1$.

The phase pressures are related to capillary pressure p_c. Capillary pressure is the difference in pressure across the interface between two immiscible fluids. In oil-water systems, water is typically the wetting phase and results in the corresponding capillary pressure $p_{cow} = p_o - p_w$. For gas-oil systems, oil is typically the wetting phase and is related to capillary pressure $p_{cgo} = p_g - p_o$. [4]

For a black-oil model, it is often suitable to work with the conservation equation of standard volumes instead of the conservation equation of mass. The mass fraction of the gas components in the oil phase can be determined by the so-called dissolved gas-oil ratio R_{SO}. The subscript s denotes that variables are measured under standard surface conditions. In case of V_{Gs}, s describes the volume of gas at standard conditions, at a given pressure and reservoir temperature, dissolved in a volume of stock tank oil V_{Os} . [4]

$$R_{SO}(p, \mathbf{T}) = \frac{V_{Gs}}{V_{Os}} = \frac{W_g \rho_{os}}{W_o \rho_{gs}} \tag{2-22}$$

The Formation Volume Factor for oil B_o is the ratio of the volume of the oil phase V_o, measured at reservoir conditions to the volume of the oil component V_{os}, measured at standard conditions.

$$B_o(p, \mathbf{T}) = \frac{V_o(p, t)}{V_{os}} = \frac{(W_o + W_g)\rho_{os}}{W_o \rho_o} \qquad (2\text{-}23)$$

where W_o and W_g are the weights of the oil and gas components, respectively. Considering the mass fractions of the oil and gas components of the oil phase, equation (2-22) and (2-23) lead to:

$$\rho_o = \frac{R_{So}\rho_{gs} + \rho_{os}}{V_{gs}} \qquad (2\text{-}24)$$

According to equation (2-23) the gas Formation Volume Factor B_g is defined by:

$$B_g(p, \mathbf{T}) = \frac{V_g(p, t)}{V_{gs}} = \frac{\rho_{gs}}{\rho_g} \qquad (2\text{-}25)$$

And the Formation Volume Factor for water is defined by:

$$B_w = \frac{\rho_{ws}}{\rho_w} \qquad (2\text{-}26)$$

Substituting equations (2-24), (2-25) and (2-26) into equations (2-18), (2-19) and (2-20) yields to the conservation equations on standard volumes

for water:

$$\frac{\partial}{\partial t}\left(\frac{\phi \rho_{ws} S_w}{B_w}\right) = -\nabla \cdot \left(\frac{\rho_{ws}}{B_w}\mathbf{u}_w\right) + q_W \qquad (2\text{-}27)$$

for oil:

$$\frac{\partial}{\partial t}\left(\frac{\phi \rho_{os} S_o}{B_o}\right) = -\nabla \cdot \left(\frac{\rho_{os}}{B_o}\mathbf{u}_o\right) + q_o \qquad (2\text{-}28)$$

and for gas:

$$\frac{\partial}{\partial t}\left(\phi\left(\frac{\rho_{gs} S_g}{B_g} + \frac{R_{so}\rho_{gs} S_o}{B_o}\right)\right) = -\nabla \cdot \left(\frac{\rho_{gs}}{B_g}\mathbf{u}_g + \frac{R_{so}\rho_{gs}}{B_o}\mathbf{u}_o\right) + q_g \qquad (2\text{-}29)$$

All three conservation equations (2-27), (2-28) and (2-29) are assumed under standard volumes. Therefore, the volumetric rates q_w, q_o and q_g are also given at standard conditions:

$$q_w = \frac{q_{ws}\,\rho_{ws}}{B_w}, \qquad q_o = \frac{q_{os}\,\rho_{os}}{B_o}, \qquad q_g = \frac{q_{gs}\,\rho_{gs}}{B_g} + \frac{q_{os}\,R_{so}\,\rho_{gs}}{B_o} \qquad (2\text{-}30)$$

The densities under standard condition ρ_{ws}, ρ_{os} and ρ_{gs} are constant.

Furthermore, two additional properties have to be introduced. First, fluid gravity γ_α for all three phases is introduced:

$$\gamma_\alpha = \rho_\alpha g \qquad \alpha = w, o, g. \qquad (2\text{-}31)$$

Next the transmissibility T of the fluid is defined by:

$$T_\alpha = \frac{k_{r\alpha}}{\mu_\alpha B_\alpha}\,\bar{k} \qquad \alpha = w, o, g. \qquad (2\text{-}32)$$

where $k_{r\alpha}$ defines the relative permeability, μ_α the viscosity, and B_α the Formation Volume Factor for the phase α.

Substituting equation (2-30), (2-31) and (2-32) into equation (2-27), (2-28) and (2-29), and dividing the resulting equations by ρ_{ws}, ρ_{os} and ρ_{gs}, respectively, we obtain the following equations under standard conditions: equation:

for water
$$\frac{\partial}{\partial t}\left(\frac{\phi S_w}{B_w}\right) = \nabla \cdot (T_w[\nabla p_w - \gamma_w \nabla z]) + \frac{q_{w_s}}{B_w}, \qquad (2\text{-}33)$$

for oil:
$$\frac{\partial}{\partial t}\left(\frac{\phi S_o}{B_o}\right) = \nabla \cdot (T_o[\nabla p_o - \gamma_o \nabla z]) + \frac{q_{o_s}}{B_o}, \qquad (2\text{-}34)$$

and for gas:

$$(2\text{-}35)$$

$$\frac{\partial}{\partial t}\left(\phi\left(\frac{S_g}{B_g} + \frac{R_{so}S_o}{B_o}\right)\right) = \nabla \cdot \left(T_g[\nabla p_g - \gamma_g \nabla z] + R_{so}T_o[\nabla p_o - \gamma_o \nabla z]\right) + \frac{\rho_{gs}}{B_g} + \frac{R_{so}\,q_{os}}{B_o}$$

2.4.2   Basic Differential Equation of a Black-Oil Model for Component Oil

This subchapter goes a little further into the mathematical background of this thesis and the applied solver.

Substituting equations (2-31) and (2-32) into equation (2-34) will lead to:

$$\nabla \cdot \left(\frac{k_{ro}}{\mu_o B_o} \bar{k} \cdot [\nabla p_o - \rho_o g \nabla z] \right) + \frac{q_{os}}{B_o} = \frac{\partial}{\partial t} \left(\frac{\phi S_o}{B_o} \right) \qquad (2\text{-}36)$$

Equation (2-36) represents component oil in a multi-phase displacement system.

Following boundary conditions are assumed:

- The water-oil-contact is in far lower regions than the reservoir; hence no initial water saturation $S_{wi} \rightarrow S_w = 0$ can be expected within the reservoir.

- There exists only a liquid undersaturated oil phase. The oil-phase is also assumed to be slightly compressible at the beginning, to introduce the Formation Volume Factor of oil B_o. Later phase compressibility will be neglected to deal with an incompressible oil phase, which leads to a constant Formation Volume Factor of $B_o = 1$.

- There is no free gas in the reservoir, nor in the vicinity of the wellbore during production. Hence, there is no immobile or mobile gas saturation within the reservoir $S_{gi} \rightarrow S_g = 0$.

All test cases and the solver in this thesis are designed to process an incompressible, single-phase flow through a compressible porous media, which is saturated only by that single phase. These assumptions will strongly simplify the black-oil formulation. [1] [2] [26]

2.5 Flow Equation for Incompressible Fluid - Compressible Rock

The next step would be to cancel negligible terms of Equation (2-36), such as the saturation S, Formation Volume Factor B, and relative permeability k_r, according to assumption made in chapter 2.4.2. Further, to adapt the single phase equation (2-36) to a 3D environment Darcy's velocity (2-7) for a 3D flow system is introduced. Hence, substituting the simplified form of equation (2-7) into (2-16) yields:

$$\frac{\partial}{\partial t}(\phi\rho) = \nabla\left(\frac{\rho}{\mu}\bar{k}\cdot(\nabla p - \rho g\nabla z)\right) + q \tag{2-37}$$

Additionally to chapter 2.1: it is sometimes possible to assume that the rock compressibility c_R in a reservoir is constant over a certain pressure range. After integration of equation (2-1) the porosity ϕ can be expressed as:

$$\phi = \phi^0 e^{c_R(p-p^0)} \tag{2-38}$$

where ϕ^0 is the porosity at a reference pressure p^0. The reference pressure p^0 is usually the atmospheric pressure or the initial reservoir pressure.

Using a Taylor series expansion, leads to:

$$\phi = \phi^0\left\{1 + c_R(p-p^0) + \frac{1}{2!}c_R{}^2(p-p^0)^2 + \frac{1}{3!}\ldots\right\} \tag{2-39}$$

An approximation of this Taylor series in equation (2-39) will result in the simplified equation for porosity:

$$\phi \approx \phi^0\left(1 + c_R(p-p^0)\right) \tag{2-40}$$

Considering the compressibility factor in equation (2-2), it follows:

$$\frac{d\phi}{dp} = \phi^0 c_R \tag{2-41}$$

After carrying out the time differentiation on the left hand side of equation (2-19), this equation becomes:

$$\left(\phi\frac{d\rho}{dp} + \rho\frac{d\phi}{dp}\right)\frac{\partial p}{\partial t} = \nabla\left(\frac{\rho}{\mu}\bar{k}\cdot(\nabla p - \rho g\nabla z)\right) + q \tag{2-42}$$

Since the fluid is assumed to be incompressible, the density ρ of the fluid remains constant. Considering this and substituting (2-41) into equation (2-42) leads to:

$$(\phi^0 c_R)\frac{\partial p}{\partial t} = \nabla\left(\frac{\rho}{\mu}\bar{k}\cdot(\nabla p - \rho g\nabla z)\right) + q \tag{2-43}$$

The flow term of equation (2-43) can be rewritten as the following:

$$\nabla\left(\frac{\rho}{\mu}k\cdot\nabla p - \frac{\rho}{\mu}\bar{k}\cdot\rho g\nabla z\right) = \nabla\left(\frac{\rho}{\mu}\bar{k}\cdot\nabla p\right) - \nabla\left(\frac{\rho^2\bar{k}g}{\mu} - \begin{pmatrix}0\\0\\z\end{pmatrix}\right) \tag{2-44}$$

Additional to the constant fluid density ρ, the fluid viscosity remains constant. The permeability k also remains constant within a grid-block.

This will simplify equation (2-44), since the constant gravity term can be replaced, using a constant value of the corresponding overburden-pressure. Considering this, equation (2-43) will lead to:

$$(\phi^0 c_R)\frac{\partial p}{\partial t} = \nabla\left(\frac{\rho}{\mu}\bar{k}\cdot\nabla p^*\right) + q \tag{2-45}$$

where ∇p^* represents the pressure field needed to be discretized. Equation (2-45) consists of an accumulation term (rate of mass change) on the left side, the flow term (change in mass flux) on the right side and the production term on the very right.

An analytic solution can be obtained for strongly simplified reservoir problems. In general, a numerical solution of this equation (2-45) is intended.

2.6 Numerical Methods

The previous chapters presented basic data and equations, which are needed to describe a common reservoir problem. The next step would be a numerical approach to approximate these partial differential equations.

Discretization is defined as a numerical approximation of a problem into discrete quantities. In our case the discretization equation is an algebraic relation connecting the values of the wanted pressure to a group of grid-points, which will be adduced later in equation (2-52). This discretization equation is derived from the differential equation and expresses the same physical information as the differential equation. Thereby, the wanted pressure value at a grid point will influence the pressure only in its immediate neighborhood. [37]

The arising partial differential equations, which describe the mathematical model, have to be solved analytically by replacing them with simple algebraic equations toward making them suitable for numerical evaluation. [4] Therefore, it is necessary to treat the reservoir as if it were composed of discrete volume elements and to compute changes within each volume element over discrete time intervals. [34]

There exist several methods to discretize a problem:

- Finite Volume Method (FVM) [35]

- Finite Element Method (FEM) [35]

- Finite Difference Method (FDM) [4]

For this thesis Finite Volume Method is chosen, since it is applicable to unstructured and complex meshes and therefore applied in many CFD programs. Basics of this approach are based on literature of OpenFOAM, such as "OpenFOAM User Guide" [12] and "OpenFOAM Programmers Guide" [17].

2.6.1   Finite Volume Method (FVM)

The name "Finite Volume" refers to the generated small volume, a so-called control cell, surrounding each node point on a mesh. To visualize the structure of such volume field, the mesh is simplified to a 2 dimensional, rectangular grid-net, which is shown in Figure (2-5).
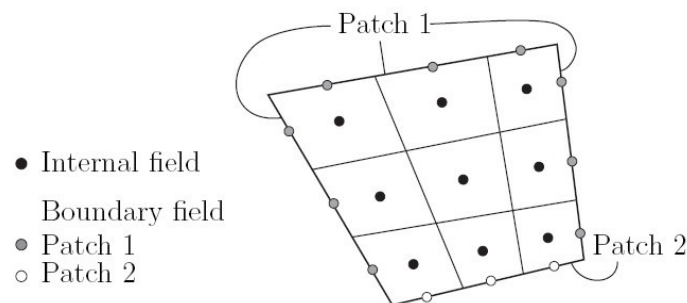
Figure 2-5: Cell centre field [17]

The data is therefore stored at the grid point "Internal field" in Figure 2-5, at the center of a "control volume", bounded by Patch 1 and 2.

The Finite Volume Method consists of static functions, representing differential operators, such as ∇, ∇^2 and $\partial/\partial t$ to discretize the geometric field and is usually applied to calculate implicit derivatives and finally return a matrix. The Finite Volume Method discretizes the problem as follows: [17]

1. Spatial discretization defines the solution domain by a set of points that fill and bind a region of space when connected. As a result, the space domain is filled by small control cells, which can be seen in Figure 2-6.

2. Temporal discretization divides the time domain into a finite number of time intervals and can be seen in Figure 2-6.

3. Equation discretization finally generates a system of algebraic equations in terms of discrete quantities defined at specific locations in the domain, from the partial differential equations that characterize the problem. [17]

A schematic illustration of spatial and temporal discretization can be seen in Figure 2-6.
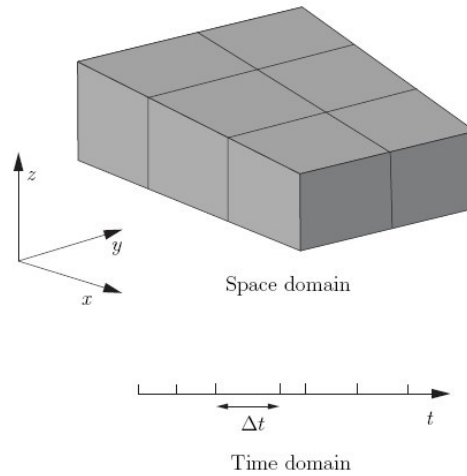
Figure 2-6: Discretization of the solution domain [17]

The flow through boundaries of spatial cells is based on flow equation (2-45). It can be assumed, that the permeability remains isotropic within a single grid-block. Hence, all control cells occupying the same grid block can be referred to the absolute permeability k. Considering this, equation (2-45) will finally lead to:

$$\nabla^2 p^* = \frac{\phi^0 \mu c_R}{k} \frac{\partial p}{\partial t} \qquad (2\text{-}46)$$

Equation (2-46) is the equation for a single phase filtration of an incompressible fluid of constant density and constant viscosity through a compressible permeable domain. [17] [6]

The arising piezometric or hydraulic conductivity "Dp" within a control volume is introduced as:

$$Dp = \frac{k}{\phi^0 c_R \mu} \qquad (2\text{-}47)$$

Dp defines the transport properties and potential of the reservoir and is formulated as pressure scalar.

Substitution of equation (2-47) into equation (2-46) leads to the equation to be spatially discretized:

$$\frac{\partial p}{\partial t} = \nabla(Dp \cdot \nabla p^*) \qquad (2\text{-}48)$$

Spatial discretization refers to a process of dividing the reservoir domain in space into a number of cells and thereby modeling the flow by a numerical method. A typical cell and its neighboring cells are shown in Figure 2-7. [17] [37]
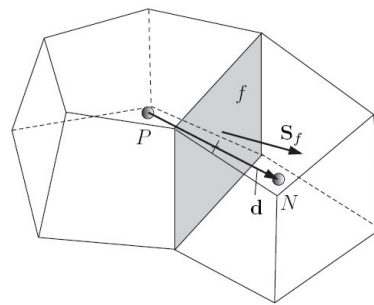
Figure 2-7: Parameters in finite volume discretization [17]

Computational nodes (P and N), so-called grid points are set at the centre of the cells and denote the point in space where pressure, velocity and other dependent variables are stored. The cells are bound by a set of flat faces f. S_f represents the surface area vector. Interpolation is used to express variable values at the cells surface in terms of the centered nodal value. Cells do not overlap with their neighbors and completely fill the domain. In OpenFOAM there is no fixed value of faces bounding each cell, no restriction on the alignment of each face and no required shape of a cell. This kind of mesh is often referred to as "arbitrarily unstructured". Codes with arbitrarily unstructured meshes offer greater freedom in mesh generation and manipulation in particular when the geometry of the domain is complex or changes over time. The ability of handling unstructured meshes will be a future advantage of OpenFOAM over commercial software, for near wellbore simulation. [17] [37]

Finite Volume Method discretization of each term is formulated by first integrating the term over a cell volume V. Most spatial derivative terms are then converted to integrals over the cell surface S bounding the volume using Gauss's theorem and is finally defined by: [17]

$$\iiint_V \nabla(\Gamma \nabla \vartheta) \cdot dV = \iint_S dS \cdot (\Gamma \nabla \vartheta) = \sum_f \Gamma_f S_f \cdot (\nabla \vartheta)_f \qquad (2\text{-}49)$$

where Γ, ϑ can represent any tensor field, such as the pressure tensor field Dp of equation (2-48). Inserting equation (2-48) into (2-49) leads to the spatial discretization:

$$\iiint_V \nabla(Dp \cdot \nabla p) \cdot dV = \iint_S dS \cdot (Dp \cdot \nabla p) = \sum_f Dp_f S_f \cdot (\nabla p^*)_f \qquad (2\text{-}50)$$

The right hand side is the Laplacian term integrated over a control volume.

The face gradient discretization in Figure 2-7 is implicit if the length vector d between the centre of the cell of interest P and the centre of a neighboring cell N is orthogonal to the face S_f. If this is the case, equation (2-51) is valid. [17]

$$S_f \cdot (\nabla p)_f = |S_f| \frac{p_N - p_P}{|d_{PN}|} \qquad (2\text{-}51)$$

Temporal discretization: To find a numerical solution for the partial differential equation, discretization has to be carried out in time. The time dependent transient terms are just derivatives with respect to one independent variable: the time. In general, the transient terms describe the accumulation of a certain variable inside an infinitesimal control volume. This discretization of the transient terms is usually called temporal discretization or discretization in time. [11] [17]

The first time derivative $\partial/\partial t$ is integrated over a control volume. The general form of the time discretization is: [17]

$$\frac{\partial}{\partial t} \int_V p\vartheta \cdot dV \qquad\qquad (2\text{-}52)$$

Hereby the time is broken into a set of time steps Δt that may change during numerical simulation. The following time steps are necessary: [17]

- New values: $p^n \equiv p(t + \Delta t)$ at the solving time step.

- Old value: $p^0 \equiv p(t)$ time step, which is stored from the previous time step.

- Old-old values: $p^{00} \equiv p(t - \Delta t)$ stored from a time step previous to the last.

To provide optimal comparable simulation results, in respect to ECLIPSE, the "backward differencing scheme" [21] is applied. The backward difference scheme in equation (2-53) is of second order and accurate in time by storing the old-old values and therefore with a larger overhead in data storage than the standard Euler-implicit scheme. [17]

$$\frac{\partial}{\partial t} \int_V p \cdot dV = \frac{3(p_P V)^n - 4(p_P V)^0 + (p_P V)^{00}}{2\Delta t} \qquad\qquad (2\text{-}53)$$

<u>Equation discretization:</u> finally converts the partial differential equations into a set of algebraic equations, which can be expressed in matrix form. After spatial and temporal discretization equations (2-50 and 2-53) are combined, the following discretized equation arises: [17] [6]

$$\frac{3(p_P V)^n - 4(p_P V)^0 + (p_P V)^{00}}{2\Delta t} = \sum_f \mathrm{Dp}_f S_f \cdot (\nabla p^*)_f \qquad\qquad (2\text{-}54)$$

The next step is to consider a random-shaped control cell. In case of Figure 2-8, an eight-sided cell named "33", which is bounded in horizontal plane by six cells: 32, 34, 38, 41, 44 and 43, is created. All length vectors d_{33-X} between cell centre "33" and cell centre X

penetrate their corresponding face area vector $S_{f\ 33-X}$ orthogonal to the face plan, where subscript X represents a neighboring cell.
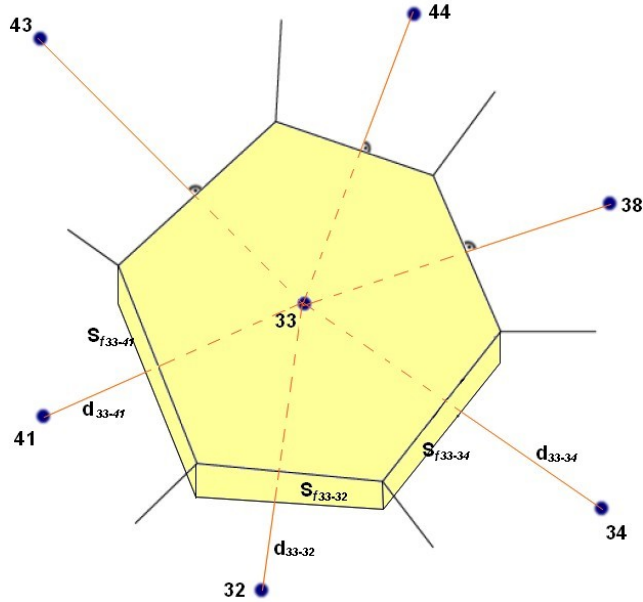
Figure 2-8: Typical relationship between discretized cells

Using algorithm (2-51), equation (2-52) for cell number "33" at the fourth discretization time-step "t4", can be written as the following:

$$V_{33} \frac{3(p_{33})^{t4} - 4(p_{33})^{t3} + (p_{33})^{t2}}{2\Delta t} = \tag{2-55}$$

$$= |S_{33-32}| \cdot \frac{p_{32} - p_{33}}{|d_{33-32}|} + |S_{33-34}| \cdot \frac{p_{34} - p_{33}}{|d_{33-34}|} + |S_{33-38}| \cdot \frac{p_{38} - p_{33}}{|d_{33-38}|} +$$

$$+ |S_{33-41}| \cdot \frac{p_{41} - p_{33}}{|d_{33-41}|} + |S_{33-43}| \cdot \frac{p_{43} - p_{33}}{|d_{33-43}|} + |S_{33-44}| \cdot \frac{p_{44} - p_{33}}{|d_{33-44}|} + \cdots$$

For completeness, bottom and top cells have to be added to complete cell "33".

2.7 Initial and Boundary Conditions

So far the mathematical model describing a single phase flow is not complete. Matching boundary and initial conditions have to be formulated.

2.7.1 Initial conditions

In general, an initial reservoir pressure is given as a reference pressure at a reference depth. The pressures at other locations in the reservoir are computationally calculated by the use of gravity equilibrium conditions [4]. However, static conditions, which remain constant, such as permeability and porosity, have to be specified at the initial time-step.

2.7.2 Boundary conditions

Reservoir models have to capture the reservoir in its whole major dimensions to predict all aspects of the true flow behavior. Therefore boundary conditions on all boundary faces of the meshed reservoir model have to be specified to keep the simulation robust and reliable. When performing discretization of terms that include the sum over faces $\sum_f$, certain exceptions have to be considered, for example if one of the faces is a boundary face. [17] Boundary conditions can be divided into two types:

- Dirichlet type, which specifies the value of the dependent variable on the boundary and is describable as 'fixed value' or boundary conditions of the first kind. [17]

- Neumann type, which specifies the gradient of the variable normal to the boundary and is termed as 'fixed gradient' or second kind of boundary conditions. For example, Neumann boundary condition arises if a constant flow rate describes the flow across cell boundaries. [17] [4]

Production scenarios: The numerical simulation of single-phase flow must account for the treatment of wells. As an approximation it can be considered that isolated production, cells (well-blocks) are mass sinks for the fluid. These production cells drain the reservoir and

therefore, require a specific treatment. To simplify the production procedure perforated wellbore intervals are labeled as "production cells" and production settings are assigned one-on-one to the outer boundaries of these cells. [4]

The outer boundaries of the cell restrict the oil production from neighboring cells according to a target production scenario. This could be either a constant production rate or a constant bottom hole pressure (BHP).

- Constant production rate allows a defined, constant oil rate, [volume per time], to flow through cell boundaries. This boundary condition can be attributed to the fixed pressure gradient: Neumann type.

- Constant BHP: The flow rate is restricted in terms of a constant pressure at the boundary. Therefore, the well production or injection is the sum of the implicit flow, from or to the neighboring cells. Since the pressure is set to a fixed value the changes must be zero: Dirichlet type.

Outer boundary of the reservoir: In practice, the permeable reservoir rock is usually bounded by no-flow layers of clay, shale or other impermeable sediments. Consequently, the fluid within the reservoir is not allowed to flow across theses external boundaries. [34] The following assumptions are valid for all three test-cases in chapter 5:

- All six sides of the reservoir are bounded by a no flow boundary (type wall).

- Test cases exhibit neither additional faults nor no-flow areas.

- Since the reservoir is assumed to be fully closed, there is no possible contact with a low lying aquifer, meaning that there is no additional driving force such as a streaming-in water-phase.

Next to the listed boundary conditions, flow behavior is further affected by additional conditions, such as fracture treatment, faults and well configurations. [4] These features of a natural occurring reservoir are neglected in all three test cases in order to keep the simulation simple and avoid unnecessary error sources.

3. Introduction to Compared Simulation Software

Reservoir simulators are built on reservoir models that include the petrophysical characteristics required to understand the behavior of the fluids over time. [9] The mathematical formulae of chapter 2 are basis for a single phase, black-oil model and can be implemented into an OpenSource CFD-software to predict future reservoir production and pressure distribution under a series of potential scenarios, such as drilling new wells, closing exiting wells or performing various production scenarios. [9]

For this reason, OpenFOAM [12] is chosen, to present the potential of modern OpenSource software in the field of reservoir simulation. A brief introduction of the structure of OpenFOAM in chapter 3.1 will lead to the presentation of the PRSFoam solver and possible reservoir simulation applications.

To perform a meaningful comparison it is necessary to simulate with a reliable, well-known commercial counterpart, such as Schlumbergers ECLIPSE [22]. Therefore, chapter 3.2 will give a short introduction into the structure and operation of the ECLIPSE_100 solver [22].

3.1 OpenSource Software OpenFOAM [12]

In 2004 an ambitious community of interest established the OpenSource "Computational Fluid Dynamic" (CFD) tool "Open Field Operation and Manipulation", short "OpenFOAM". This software is able to simulate complex fluid flow models, including chemical reactions, turbulences, heat transfer, solid dynamics and electromagnetism. OpenFOAM was introduced by OpenCFD Ltd. and is released under the General Public License (GPL), which is a widely used free software license. In general, the simulation of fluid dynamic models requires highly developed software programs and hardware components. Both attributes improved within the last couple of years, allowing CFD simulations to challenge the position of expensive and time consuming experiments.

In comparison to commercial software tools, OpenFOAM is characterized as OpenSource, meaning that the source code is not restricted and can be modified by the user. The core of OpenFOAM is formed by a library, written in the C++ programming language. The OpenSource library can be processed, meaning that the user is free to create new applications or upgrade existing ones. The set of precompiled libraries is dynamically linked during compilation of the solvers and utilities. These applications can be split in two categories:

- Solvers, which are used to solve specific problems in engineering mechanics.

- Utilities, which are necessary to perform pre- and post-processing tasks, involving data manipulations and algebraic calculations, such as mesh visualization and mesh processing.

Since the release of OpenFOAM a large number of applications have appeared on CFD platforms. Additionally to these solvers and utilities, OpenFOAM is also supplied with a plugin (paraFoam) to visualize solution data and meshes are shown via ParaView, which will be discussed in chapter 3.1.3. Additionally, a wide range of mesh converters allows its user to import meshes of leading commercial software packages, such as FLUENT [19] or CAD. [12] [17]

The overall structure of OpenFOAM can be seen in Figure 3-1.
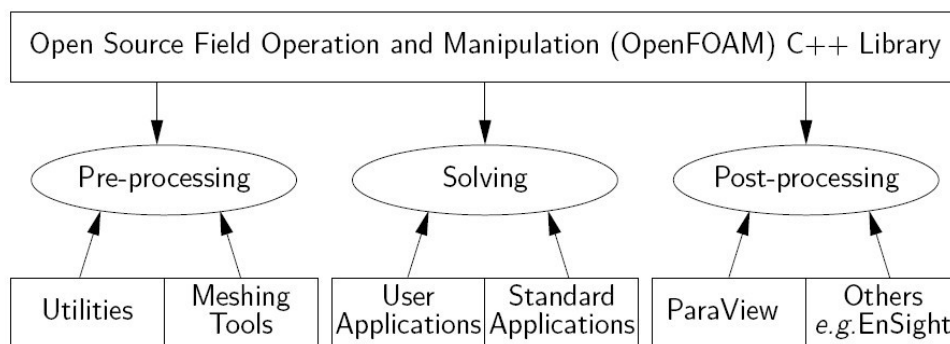
Figure 3-1: Overview of OpenFOAM structure

Apart from available standard solvers, OpenFOAM offers the possibility to create additional custom solver applications.

All simulation data should be collected and stored in a case folder, labeled with a simple, significant name. The standard structure of such <case> folder can be seen in Figure 3-2.
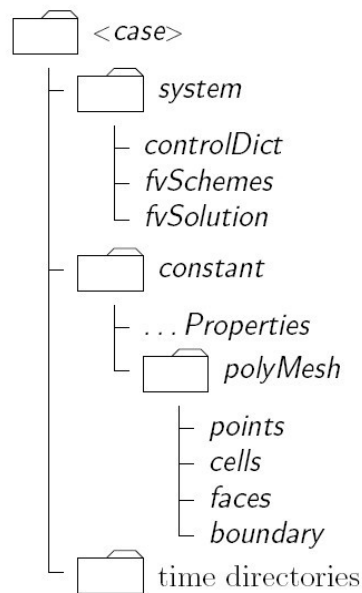
Figure 3-2: Case directory structure [15]

When a case is started, the solver will pick up all the information needed to proceed. Cases should include the following initial three subdirectories: time "0" time directory, "system" and "constant":

"0" time directory: This directory represents the initial conditions of simulation at time-step 0. The folder includes case data such as initial values and boundary conditions. During a simulation run, all results of dynamic properties are written to data files and stored in an additional corresponding "time" folder.

"constant": This directory contains settings and descriptions of the case mesh and physical properties required for the simulation run. For the used PRSFoam solver, the directory "constant" includes the following files:

- "mechanicalProperties" text file containing data of physical fluid and rock properties, such as viscosity, density, E-Module, etc.

- "transportProperties" including properties such as reference pressure, reference depth, stress analyses etc.

- "thermalProperties" containing temperature field variables, such as thermal stress analyses, etc.

- "polyMesh" containing a full description of the reservoir mesh. This includes information about boundaries, neighbours, points, owners, faces, etc.

"system": This directory stores settings describing the simulation workflow. It contains parameters such as time-management, discretization and solution schemes. The folder includes at least the following files:

- "controlDict" contains the time dependent control check-up and writing adjustment; this includes simulation start time, end time, time step lengths, data output interval, etc.

- "fvSchemes" dictionary sets discretization schemes for terms, such as derivatives in equations that appear in applications being run. For example, the first time schemes ddtSchemes, gradSchemes, laplacianScheme, etc.

- "fvSolution" contains keywords defining the type of solver that is used to solve appearing pressure- and velocity equations. It also includes a PISO [12] sub-dictionary for algorithm control. [12] fvSolution also defines the preconditioner of matrices: "GAMG" [12] preconditioner uses the principle of generating a quick solution on a mesh with a small number of cells, then mapping this solution onto a finer mesh and finally using it as a first estimation to obtain an accurate solution on the refined mesh, making GAMG faster than other methods. [12]

3.1.1 Structure of OpenFOAM for Reservoir Tasks

After completing a simple ECLIPSE case study, all properties and mesh files have to be converted into an OpenFOAM readable structure. Therefore the converter *"ECL2FoamGrid"* is introduced to translate ECLIPSE cases, written in FORTRAN to OpenFOAM's C++ structure, so that they can be used for further calculation. These transformed data files are stored unstructured in the initial ECLIPSE file and have to be allocated into appropriate time directory *"0"* or *"polyMesh"* folder.

The initial time folder *"0"* will contain data files of static properties such as well position, reservoir depth, rock characteristics and all grid block information. In detail:

- DEPTH   Lists depth of each block

- J-, I-, K-INDEX   Sets block position in x, y, z direction

- muO   Definition of the average fluid viscosity

- PERMX, -Y, -Z   Permeability of each block in the reservoir

- PORO   Porosity of each block in the reservoir

- wellDict   Definition of position and production conditions of each well

- p   Initial pressure for each block

- T   Reference temperature at reservoir depth

- D   Definition and position of outer boundaries

Additionally to converted data-files, *"wellDict"* has to be modified by the user itself. It stores all essential properties associated with deployed wells and production.

The folder *"polyMesh"* has to include the converted *boundary, faces, neighbour, owner* and *points* data files to obtain a full structured and meshed reservoir.

The definition of production-wells is necessary to produce hydrocarbons. According to simulation perspective, production wells initialize the pressure difference and reservoir flow behavior. The relation between the small well diameter and the dimension of one block in

this system requires additional grid refinement and hence a higher simulation effort. To simplify this simulation, the theory of "Mass Balance" can be utilized. This means that the amount of oil which leaves through the well has to enter the outer boundary of the production block. Therefore it can be assumed that the entire perforated block is a producer and there is no need to refine the grid around a well.

A standard well description of a test case (TESTCASE_1) is presented in the following:

wells	*1*
{	*2*
well_1	*3*
{	*4*
rw 0.155448;	*5*
perforatedCells (1479 2079 2679);	*6*
pressureControl no;	*7*
qsf 0.007360523;	*8*
pwf 2.00e7;	*9*
}	*10*
}	*11*

Lines 1 to 11 define a standard production well, according to PRSFoam solver.

In details:

- "*rw*" defines the well radius in meters.

- The keyword "*perforatedCells (1479   2079   2679)*" in line 6 lists all numbers of perforated blocks.

- In line 7, the production scenario is defined. In this case it is set to a constant rate "*pressureControl no*" of "*qsf*" 7.36-E4 [m³/s], which is defined in line 8.

- If the users change "*pressureControl no*" to "*pressureControl yes*", in case of line 9 the well will start to produce with a constant BHP of 200 [bar] (pwf 2.00+E7 is defined in [kg/ms²]).

3.1.2   OpenFOAM solver PRSFoam

To process a reservoir problem based on OpenSource software OpenFOAM, the so-called PRSFoam solver was developed by HOL GmbH. The mathematical background for this solver can be seen in detail in chapter 2. To simplify the requirements for this new OpenFOAM approach to solve reservoir problems, most important conditions are repeated:

- The oil saturation is 100%, meaning that no other phase exists in this reservoir.

- There is no liberated gas at initial state and during production.

- Closed outer boundaries (physical wall), means that no additional driving force is acting on the reservoir, such as water-drive.

- The liquid phase is incompressible, meaning that the "Formation Volume Factor" (FVF) is also negligible.

This eases the black-oil equation to a one-phase-model, which is then be solved by PRSFoam. This reservoir solver picks relevant properties, such as viscosity, porosity, rock-compressibility and the initial pressure, arranges them and finally solves each node at each time step.

A short introduction into PRSFoam and the most important files and its function are presented:

- The main code of the solver is stored in the file *"PRSFoam.C"*. This file introduces all important properties, such as the mesh structure, transport properties, mechanical properties, time steps and exit conditions. Thereafter the pressure equation in *"pEqn.H"* is solved and dynamic properties are updated for the next time step. *"PRSFoam.C"* defines the simulation workflow and represents the heart of the solver.

- *"createFields.H"* defines all important fields applied in the solver. The pressure at the reference depth and the overburden gradient are used to calculate the pressure for every block at a higher or lower reference depth. Furthermore *createFields.H* is responsible for creating the volume tensor field of the permeability and imports the

porosity and the viscosity for each block. Finally the compressibility factor of the rock is introduced, which is dependent on the pressure and therefore on the block depth.

- *"pEqn.H"* solves the pressure equation for each grid block and time step. Equation (2-45) is integrated into the PRSFoam in form of:

$$\nabla \left(\frac{k}{\mu_o} \right) \nabla p^* - c_R \phi \frac{\partial p}{\partial t} = 0 \qquad (3\text{-}1)$$

The next step is to "translate" equation (3-1) into C++ and link it to the OpenFOAM code of PRSFoam solver:

```
{                                                          1
    volTensorField Dp("Dp",k/muO);                         2
            fvScalarMatrix pEqn                            3
            (                                              4
            fvm::laplacian(Dp,p) -fi*cP*fvm::ddt(p)        5
             );                                            6
pEqn.solve();                                              7
            }                                              8
```

The *volTensorField* in line 2 describes the piezometric conductivity. The resulting pressure equation of equation (3-1), which can be seen in line 5, is stored in a "finite volume scalar matrix" *fvScalarMatrix*.

- The last important file in this context defines the output of the simulation. *"write.H"* aims to specify the velocity and the pressure values for each block, which will then be used as basis for calculation of the next time-step.

3.1.3   Possible Improvements for Future OpenSource Reservoir Solvers

PRSFoam is only designed to solve a single-phase displacement using an injector well and/or a production well. Presently this solver can only deal with a single-phase production and injection scenarios.

For the future development of a fully functional OpenFOAM reservoir simulator, the following enhancements need to be implemented:

- Multi-phase phase flow of water, oil and free gas [4].

- Compressible fluids in the reservoir [4].

- Solution gas-drive [1].

- Pseudo steady-state and steady-state behavior at the outer boundaries [1].

- Production abandonment rules to avoid negative pressure in the reservoir when applying a constant production rate.

- Simulation of pressure loss according to rate dependent "skin" [14]. This pressure loss in the vicinity of the wellbore is caused by turbulent flow and can be approximated by the use of an appropriate Navier-Stokes reservoir solver.

Furthermore, a graphical user interface (GUI) to manage a revised OpenSource reservoir simulator would be useful to facilitate case set-up.

3.1.4   Post-Processing via ParaView [15]

The results of OpenFOAM's reservoir simulation are pressure and velocity data-files, stored in appropriate time dictionaries. These data files can be used to plot different kinds of production graphs, or to visualize dynamic procedures within the reservoir. The main post-processing tool provided with OpenFOAM is the reader module to run with ParaView, an open-source, visualization application. [12] ParaView is a post-processing tool used to visualize two- and three-dimensional models and was first released in 2002. It is under a BSD (Berkley software distribution) "permissive free software license" of Kitware

[15] and can be used for parallel, interactive and scientific visualization. ParaView uses a Visualization Toolkit (VTK) to load data into its manageable interface. This interface is used to adjust results of each time step and visualization settings. The conversion of data files into the required VTK-files is executed by OpenFOAM via the foamToVTK command. ParaView offers state-of-the-art data processing and visualization algorithms. It also allows advanced users to construct, navigate and modify complex structures of their cases. Starting a ParaView application creates a reader object, according to memorized processing data. This is done for every stored time step and can be visualized afterwards as a sequence. [15]

In this thesis, ParaView3 was used to visualize important simulation steps of the test-cases. All relevant issues for this reservoir simulation – such as enlarging vertical axes, creating streamlines, visualization of velocity vectors or hiding impermeable blocks - are implemented. A simple comparison of OpenFOAM and ECLIPSE post-processed results is shown in Figure 3-3.
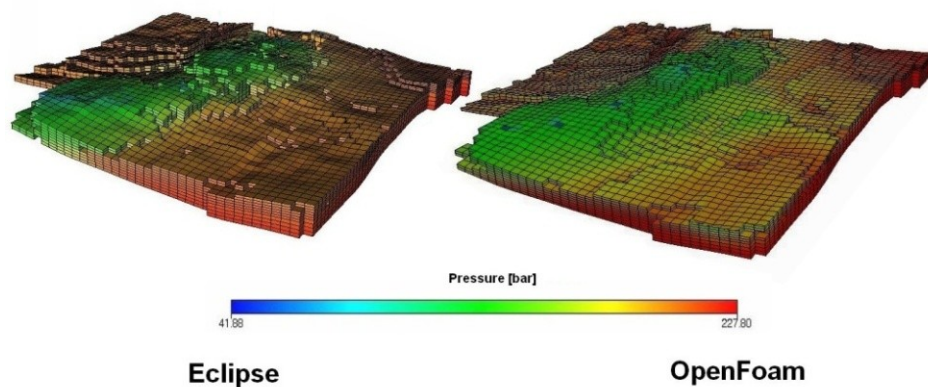
Figure 3-3: Comparison of both post-processing visualization tools

In both cases in Figure 3-3, the vertical z-direction is a fourfold higher than the original reservoir to improve visualization of the pressure distribution within the layers. Furthermore, the difference in smoothness results from the fact that both tools interpolate between blocks and light-settings of both post-processors. Yet, ECLIPSE and OpenFOAM display all test-cases without interpolated pressure performance.

Additionally to the pressure distribution, ParaView was used to show the correct position of the perforated blocks, the permeability or porosity of converted ECLIPSE reservoirs.

ParaView offers the possibility to visualize resulting velocity-streamlines. Thereby, the stream tracer filter generates streamlines in a vector field from a collection of seed points. The streamlines are generated and released if a streamline crosses a point-source or line-source boundary. The line-sourced application is used for all three test cases to demonstrate the integrity of OpenFOAM results.

A picture of resulting stream tracer of TESTCASE_1 can be seen in Figure 3-4.
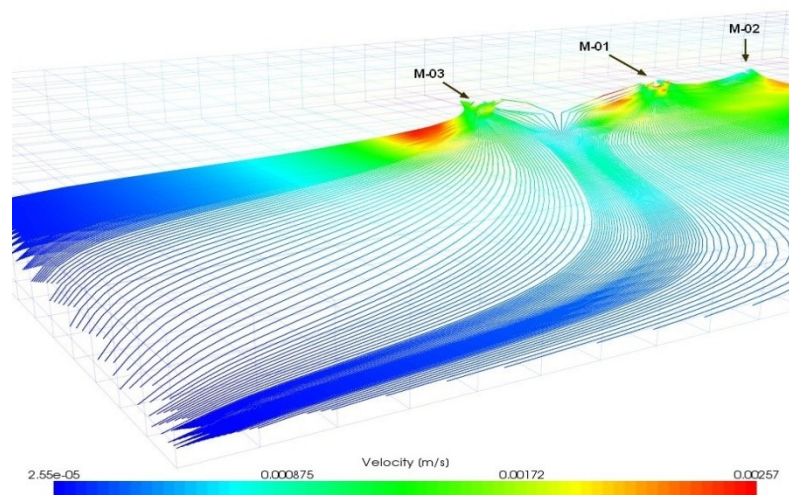
Figure 3-4: TESTCASE_1: Streamline tracer application of ParaView3 [15]

3.2 Reservoir Simulation Software ECLIPSE [22]

Schlumberger's reservoir-simulator ECLIPSE has been selected to prepare reference values of TESTCASE_1, TESTCASE_2 and test-case WATER_INJECTION. These reference values provide the opportunity to compare the resulting pressure and production-rate of OpenSource solver PRSFoam to a reliable and professional reservoir simulator.

ECLIPSE was released in the early 1990's and has evolved since then into a global standard tool for reservoir simulation. It is a costly batch software for the petroleum industry and is also used worldwide for reservoir simulation training purposes. Hence, ECLIPSE often appears in publications, simulation reference of different scientific papers and is the industries simulator benchmark.

The standard ECLIPSE simulation package includes two solvers: ECLIPSE_100, which can process so-called "black-oil models", while the ECLIPSE_300 solver supports compositional modeling. Compositional modeling can also be used in pressure maintenance operations and multiple contact miscible processes of enhanced oil recovery (EOR).

The software bundle was originally written in FORTRAN77 and can be used on desktop computers or network systems with a supported operating system and sufficient hardware resources depending on the size and complexity of the model to be processed. The wide spectrum of capabilities makes ECLIPSE a practicable simulator for dynamic modeling of reservoir with varying behavior. The input for ECLIPSE simulation can be written into free formatted ASCII text files using the ECLIPSE keyword system (suitable for simple models only) or can be prepared via a standalone pre-processing software (more common for complex reservoir geometries).

A widely known pre-processor is Schlumbergers Reservoir Characterization software package Petrel [32]. This package covers the whole reservoir characterization workflow starting from seismic interpretation, petrophysics, geological modeling, property modeling, upscaling etc. The upscaled model can then be exported to ECLIPSE interface files.

These files are structured via specific keywords and include mainly the reservoir geometry and static properties. This information forms the static grid, which is the framework for the dynamic simulation of the model.

This thesis deals with a simplified conventional recovery simulation of a single-phase, under-saturated oil reservoir and will therefore be processed with the ECLIPSE_100 solver. [9][10][22]

3.2.1   ECLIPSE 100

To complete the introduction, reference reservoir simulator ECLIPSE is introduced. ECLIPSE_100 provides a fully-implicit, three phases-, three dimensional- black-oil Simulator to solve different kinds of reservoir problems. The main input of an ECLIPSE simulation case is summarized in a DATA file. A complete ECLIPSE simulation DATA file includes links to other so-called "include files", which contain the bulk of the dynamic and static reservoir properties. Generally it can be split into the following main sections:

RUNSPEC – General model descriptions, such as title, start date, unit system, dimensions, phases present, etc.

GRID – Basic model geometry and various static rock properties, such as directional permeabilities, porosity, anisotropy and net to gross ratio (NTG) for each grid block.

EDIT – Modifications of calculated pore volumes, grid block centre depths, diffusivities, non-neighbouring connection and transmissibility.

PROPS – Includes property-tables of reservoir rock and fluids as functions of fluid pressures, saturations and compositions. Some of the required properties are: rock compressibility, relative permeability, capillary pressure, fluid density and viscosity, Equation of State (EOS) for compositional runs, etc.

REGIONS – In this section the grid is separated into areas of similar dynamic behaviour. Regions are linked to dynamic input tables from the SCAL or PVT sections. Other types of regions may be specified if needed.

Generally every grid block has to belong exclusively to one of the regions in order to have the proper dynamic properties assigned to it during the simulation.

SOLUTION – Includes the initial reservoir condition and each grid block's initial state, such as block pressure, phase saturations, and phase compositions.

SUMMARY – Specifies the required output for the graphic post-processor. For every specified time step various dynamic parameters can be written to an output file for later use in the simulation result evaluation.

SCHEDULE – In this section time dependant data is specified. This includes well operations such as production-injection rates, production-injection control, well constraints, historic production-injection data etc. In addition, wells can be grouped into nodes or well-groups and production-injection constrains can then be specified for such nodes.

If a user decides to interact via ECLIPSE office, the main structure of the DATA file can be opened or imported from an existing case. [22] The office-interface includes tools to visualize the grid model, change and introduce parameters, run simulations and display results. These modules are available through the Data-Manager-Module, which can be seen in Figure 3-5.
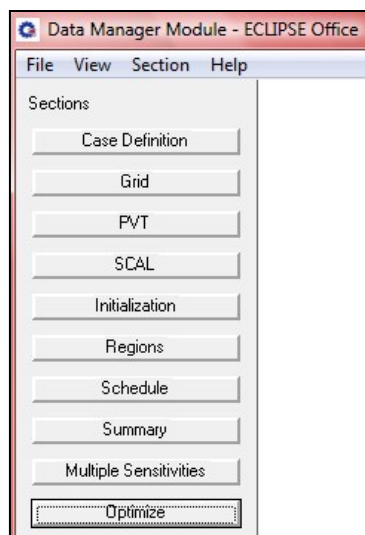
Figure 3-5: Applications of ECLIPSE Office: "Data Manager Module"

The next paragraph lists the most important control modules and introduces them briefly:

- <u>Case Definition</u> offers basic information and options to adjust the current simulation case. This includes model dimensions, type of solver, type of grid, type of geometry, phases in the reservoir, etc.

- <u>Grid</u> provides access to GRID and EDIT keywords. This option can be used to build reservoir models interactively, design grids and change grid related input data. This module offers basic options to edit contours, faults, map features, well locations and can also be used to import data directly from pre-processing map files.

- <u>PVT</u> keywords specify pressure dependent fluid properties such as Formation Volume Factor (FVF), phase viscosity, phase density and phase compressibility.

- <u>SCAL</u> "Special Core Analysis Management Software" allows for input of special core analysis data. Experimental data, like relative permeability and capillary pressure is specified in tables to characterize rock-fluid interaction.

- <u>Initialization</u> includes initial conditions such as Water Oil Contact (WOC), initial pressure and reference depth.

- <u>Regions</u> is the assignment of each grid-block to one of the PVT-, Rock-, Fluid-In-Place-, etc. regions.

- <u>Schedule</u> provides a graphical user interface to include and edit all the time dependant data for control, location and definition of all kinds of wells. A variety of different production data can be implemented or data can be extracted from existing ECLIPSE models and users can configure the type of well control, operational limits on production rates and well pressures. All important events are associated with keywords. Examples of these used to specify a production well:

    o Well Specification (WELSPEC)

    o Well Connection Data (COMPDAT)

    o Production Well Control (WCONPROD)

- <u>Summary</u> organizes and displays important keywords for all simulation results. Desired output vectors can be selected to be evaluated and displayed during and after the simulation.

- <u>Multiple Sensitivities</u>

- <u>Optimize</u> [10] [23] [22]

3.2.1 Numerical Background of ECLIPSE_100 Solver

ECLIPSE_100 contains the option for fully implicit-, IMPES- (IMplicit Pressure Explicit Saturation) and AIM- (Adaptive Implicit Method) solution methods.

- The fully implicit method is stable, reliable and may be used to solve "difficult" problems such as coning studies.

- The IMPES is less dispersive and somehow faster than the fully implicit method. It may be used on "easy" problems such as history matching applications, where the time steps are usually small.

- The AIM method for compositional studies is a compromise between fully implicit and IMPES methods. It splits the reservoir domain, allowing cells in "difficult" regions to remain in a fully implicit solution, while employing the advantage of an IMPES description in "easy" regions. This is robust and efficient for black-oil problems, generally allowing large time steps in the simulation. [9] [10]

The basic preferences of ECLIPSE "Case Definition" are set to single-phase black-oil model and fully implicit method for all three test-cases in chapter 4.

4. Test Cases

A reservoir model incorporates all the characteristics of a real or fictive reservoir that are pertinent to its ability to store and conduct hydrocarbons. These reservoir characterization models are used to simulate the behavior of the fluids within the reservoir under different sets of circumstances. [9]

In general these models are based on seismic data and reflect the structure of possible hydrocarbon reservoirs. As described in chapter 3.2, the geometry of such reservoir can be designed and structured using professional reservoir characterization software, such as Schlumbergers Petrel [32]. Resulting upscaled reservoir models can then be exported to ECLIPSE interface files and build the structure of test-cases.

To compare similar reservoir models it is necessary to use identical geometry and properties, such as permeability in x, y, and z direction, block depths and porosity for both solvers.

For this reason "ECL2FoamGrid" converter was introduced to convert existing ECLIPSE cases into OpenFOAM format. "ECL2FoamGrid" is comparable to a library. All data-files of ECLIPSE are perused, whereby relevant data and geometries are selected by the converter to structure the reservoir for OpenFOAM simulations purposes.

To prove the integrity of ECL2FoamGrid, the structure of a test-case was converted and compared., Figure 4-1 of ECLIPSE and Figure 4-2 of OpenFOAM highlight all permeable blocks in x-direction between 1 [mD] and 12 [mD]. All permeable blocks below or above this interval are suppressed in these visualizations.
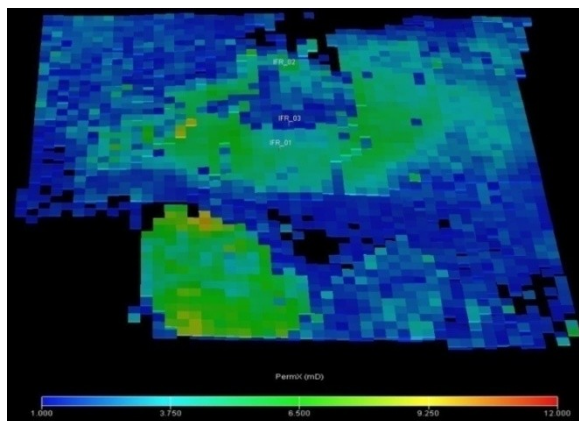
Figure 4-1: Permeable structure of ECLIPSE
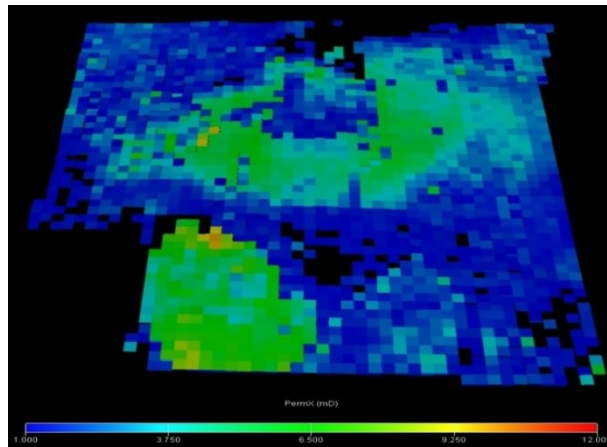
Figure 4-2: Permeable structure of OpenFOAM

From Figure 4-1, 4-2 it can seen, that both simulation tools generate the same permeable structure of the test-case.

This identically comparison result is also valid for all the other static properties of the reservoir, such as porosity, depth, block position and etc. This ensures the basis to compare different test-cases and apply different production scenarios.

To compare both solvers, ECLIPSE and PRSFoam, three test-cases were prepared: TESTCASE_1 and TESTCASE_2 each perform two different production scenarios: constant production rate and constant BHP. The third one, WATER_INJECTION represents a special test case, were a fluid is injected at the left corner, while a well in the center is producing fluid of same density as the injected one. Screenshots of all three cases can be seen in Figure 4-3.
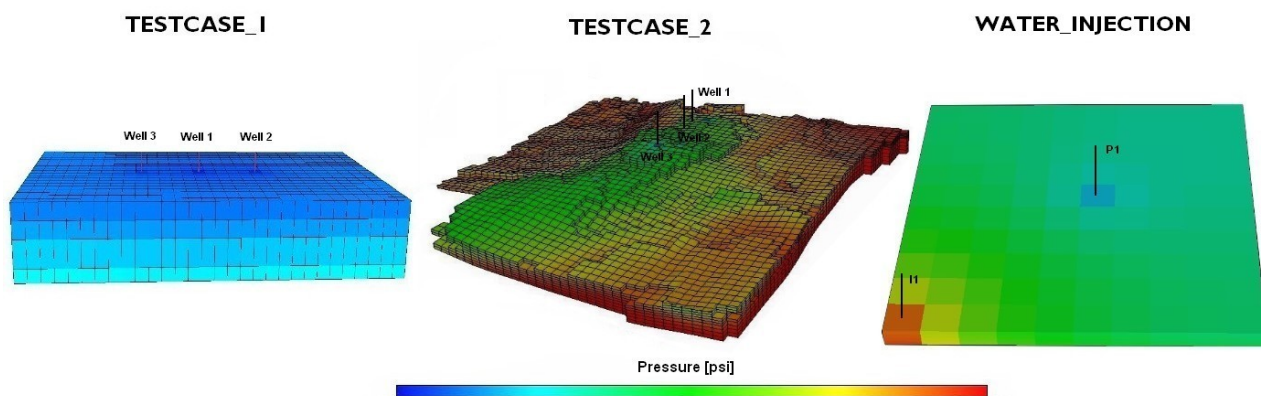
Figure 4-3: Schematic display of case TESTCASE_1, TESTCASE_2 and WATER_INJECTION

TESTCASE_1 and TESTCASE_2 are drained by three wells, which perform at identical production conditions. For the first scenario, a constant bottom hole pressure (BHP) is applied to achieve a decline in production rate, while the second scenario vice versa, will result in a BHP decline through a constant production rate.

Test-Case WATER_INJECTION is drained by one producer "P1" close to the center and one injection well "I1" in the left corner. Production and injection wells are both controlled, using a constant production and injection rate.

4.1   TESTCASE_1: Shoe Box Model

The first case, TESTCASE_1, is a simple cubic model, designed for simulation training purposes. In literature this kind of test reservoir shape is often called the "Shoe Box Model" and can be seen in Figure 4-4.

TESTCASE_1 offers a fairly large lateral expanse and its geometry and grid structure is kept as simple as possible. It is a single-phase model, containing only oil above bubble point pressure. Structurally the field consists of four almost identical permeable and porous layers. The reservoir is isolated on all sides by a closed outer boundary (type wall).
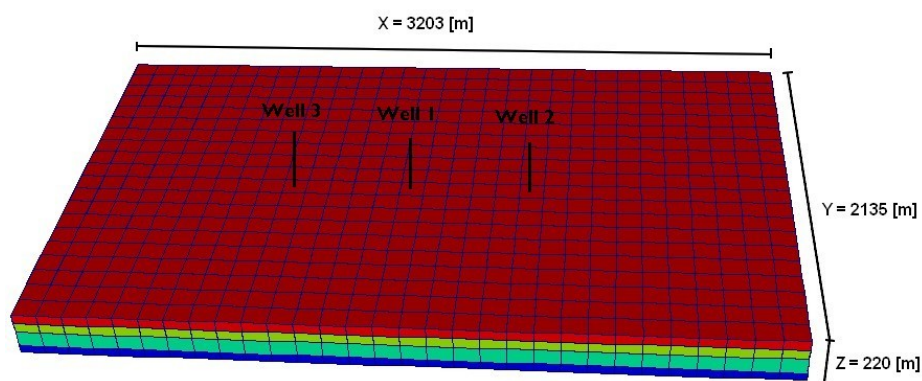
Figure 4-4: Dimensions of TESTCASE_1

To understand the OpenSource solver PRSFoam and become familiar with important parameters, the simulation of TESTCASE_1 was carried out several times under different conditions, such as different permeability, rock compressibility, porosity or well locations. According to these simulation cycles it was possible to improve the solver settings of both software tools to finally identify differences in resulting data and synchronize the workflow of ECLIPSE and OpenFOAM.

An summary of the initial and boundary conditions of TESTCASE_1 is listed in Table 4-1.

	Variables	Description	Values	Units
general properties:	TVD	reference depth	1.783,08	[m]
	t	simulated production time	4	[years]
	Δt	time interval of simulation steps	3	[days]
	Δt_{wr}	file writing interval	3	[days]
	K(z)	grid blocks in z direction	4	[blocks]
	I(x)	grid blocks in x direction	30	[blocks]
	J(y)	grid blocks in y direction	20	[blocks]
	$\sum$ grids	total sum of blocks	2.400	[blocks]
transport properties:	μ	average viscosity	0,01	[m²/s]
	p_{init}	pressure @ reference depth	230	[bar]
rock properties:	ρ	fluid density	863,6085627	[kg/m³]
	Φ	rock porosity	11 to 14	[%]
well properties:	$\sum$ well	total number of wells	3	
	r_w	well radius	0,155448	[m]

Table 4-1: Input parameter for TESTCASE_1

The following paragraph will present a brief introduction of the hydrocarbon reservoir and its dimensions.

The size of case TESTCASE_1 is defined by the following dimensions: 2.135 [m] in horizontal Y direction, 3.203 [m] in X direction and 220 [m] in vertical Z direction. These dimensions result in a total volume of 15E+8 [m³] and the OOIP of field TESTCASE_1 is approximately 16E+7 [m³] of oil. TESTCASE_1 consists of (4 x 30 x 20) 2.400 grid blocks. The Cartesian grid is therefore composed of blocks with the size 91,44 [m] x 115,82 [m] x 55,00 [m]. This leads to a total block volume of 5,82E+5 [m³].

According to the previous input data, the simulation of TESTCASE_1 is performed with both simulation tools, ECLIPSE and OpenFOAM. In Table 4-2 a comparison between ECLIPSE and OpenFOAM's wall-clock-time and the required memory is listed.

Comparison of simulation time and required memory

Processor: Intel Core2 Duo CPU P8400 @ 2.26GHz
System: 32Bit operating system

TESTCASE_1

	ECLIPSE_100	PRSFoam
Wall clock time: [s]	28	2
Required memory: [MB]	6,75	1,10

Table 4-2: TESTCASE_1: Comparison of simulation time and required memory

In this case PRSFoam performs the simulation faster and with less usage of memory than its commercial counterpart.

4.1.1 TESTCASE_1 at Constant Bottom Hole Pressure

The first simulation run was started with both programs at a constant bottom hole pressure (BHP), equal for all wells. The BHP was set to 3.000 psi at the mid-perforation.

To determine if the results of both programs are comparable, the pressure distribution after the first year and after 4 years is visualized using the ECLIPSE and OpenFOAM post-processors. In addition, the pressure data of all 3 wells for both simulators were written out and plotted.

- 52 -

At first, a scheme of the pressure distribution after the first year is shown in Figure 4-5 and Figure 4-6.
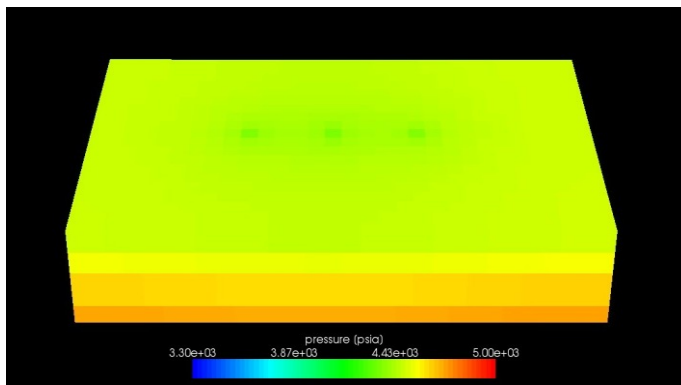
Figure 4-5: ECLIPSE result of pressure distribution after one year of production
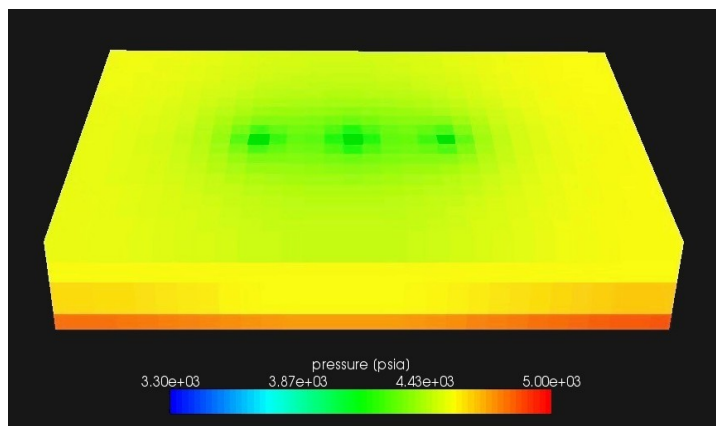
Figure 4-6: OpenFOAM result of pressure distribution after one year of production

The following pictures Figure 4-7 and 4-8, are taken after four years of constant production.
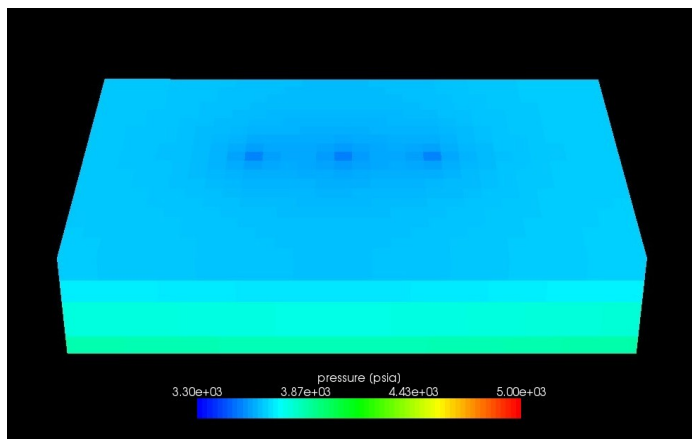
Figure 4-7: TESTCASE_1, ECLIPSE result after 4 years of production
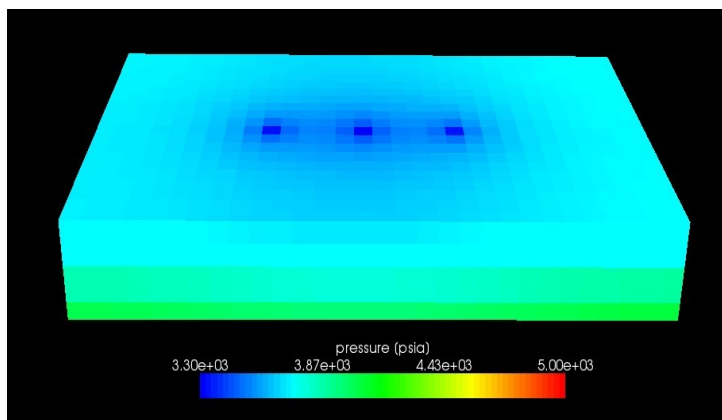
Figure 4-8: TESTCASE_1, OpenFOAM result after 4 years of production

Because of the pressure drop around all three production wells, three areas of lower pressure can be observed. The color layering, which can be observed between the different layers and around the three wells is due to the fact, that Figure 4-5, 4-6 and Figure 4-7, 4-8 show the cell value of each grid-block and not the interpolated result of the pressure

distribution in between them. The difference between ECLIPSE and OpenFOAM result from the fact that different post-processing tools used for this comparison.

Additionally to post-processed visualization, it is desirable to compare simulation results of different field- or well production over time. Screenshots just represent a single time step and it is unrewarding to present every single time step. For this reason the calculated pressure data was analyzed and plotted according to well known standard operating graphs, used in commercial reservoir engineering. In the following,

- Field performance curves

- Single well performance curves

- Daily performance curves

- Cumulative performance curves

and finally result tables of the total field performance at selective time steps will conclude this preliminary comparison between ECLIPSE and OpenFOAM.

Starting with Figure 4-9, the field performance over production time at a constant bottom hole pressure (BHP) is shown.
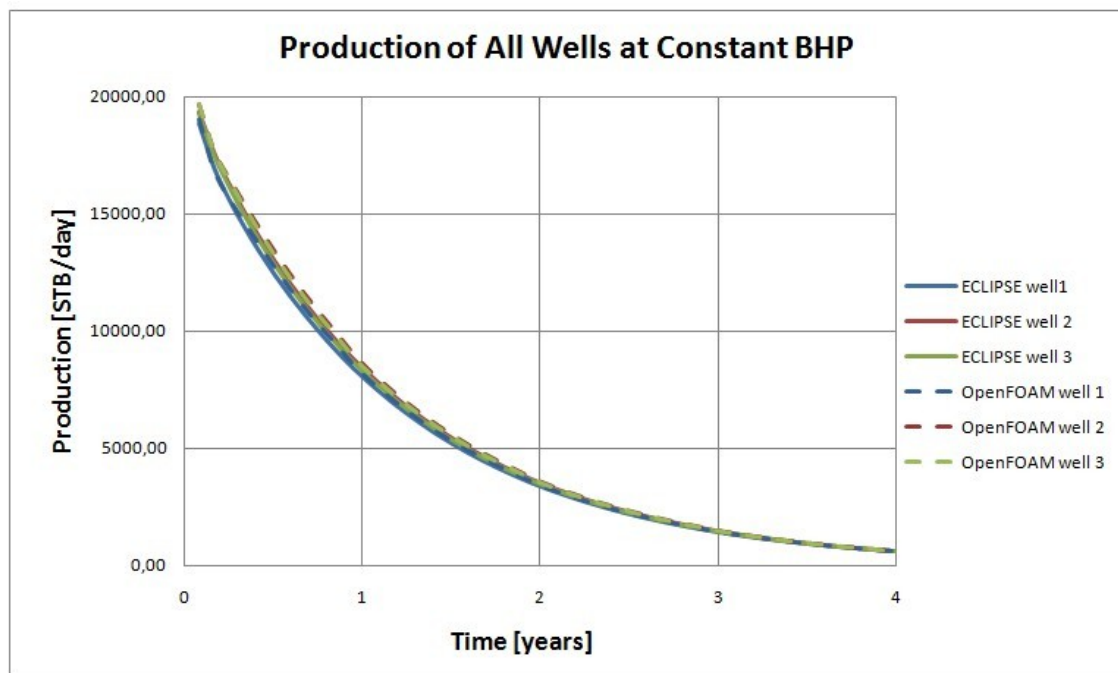
Figure 4-9: Comparison of the performance of single wells at constant BHP

As one can see, all six wells of ECLIPSE (continuous lines) and OpenFOAM (dashed lines) show same performance during the whole simulation. The similar performance of all wells results from the symmetrical structure of the reservoir TESTCASE_1, identical initial conditions for all three wells and the large distances between wells and outer boundaries. These large distances guaranty little interference between the producers.

The differences in percentage can be seen in Table 4-3.

Summary of TESTCASE_1 at constant BHP

Differences between OpenFOAM and ECLIPSE	Time-step	Well number:	[STB/day]	[%]
Max.result difference between OpenFoam and ECLIPSE	after 1 year after 4 years	#2 OpenFOAM - ECLIPSE #3 OpenFOAM - ECLIPSE	180,76 10,57	5,04 1,68
Daily production difference between ECLIPSE and OpenFoam:	after 1 year after 4 years	OpenFOAM - ECLIPSE OpenFOAM - ECLIPSE	469,04 27,63	1,85 1,48

Table 4-3: Differences of TESTCASE_1 at constant BHP

The column: "well number" lists the higher productive well first and the lower one next. This is significant in low-permeable reservoirs cases. The main reason for this obseved difference is that even for a very simplified test case, ECLIPSE will calculate using the entire set of mathematical formulae, while OpenFOAM will strictly calculate using only the simplified black-oil Model.

Most of the adaption work was done in ECLIPSE, since it was easier to follow particular relationships between variables and workflow through the GUI. On the other hand OpenFOAM emphasizes the fact, that the user can totally control operations, using an OpenSource program, while using ECLIPSE the full transparency of numerical procedure is not given.

As all three wells nearly perform identically, therefore it is sufficient to show only a comparison of one well in order to avoid unclearness. For this reason well 1 was chosen and the corresponding production graph can be seen in Figure 4-10.
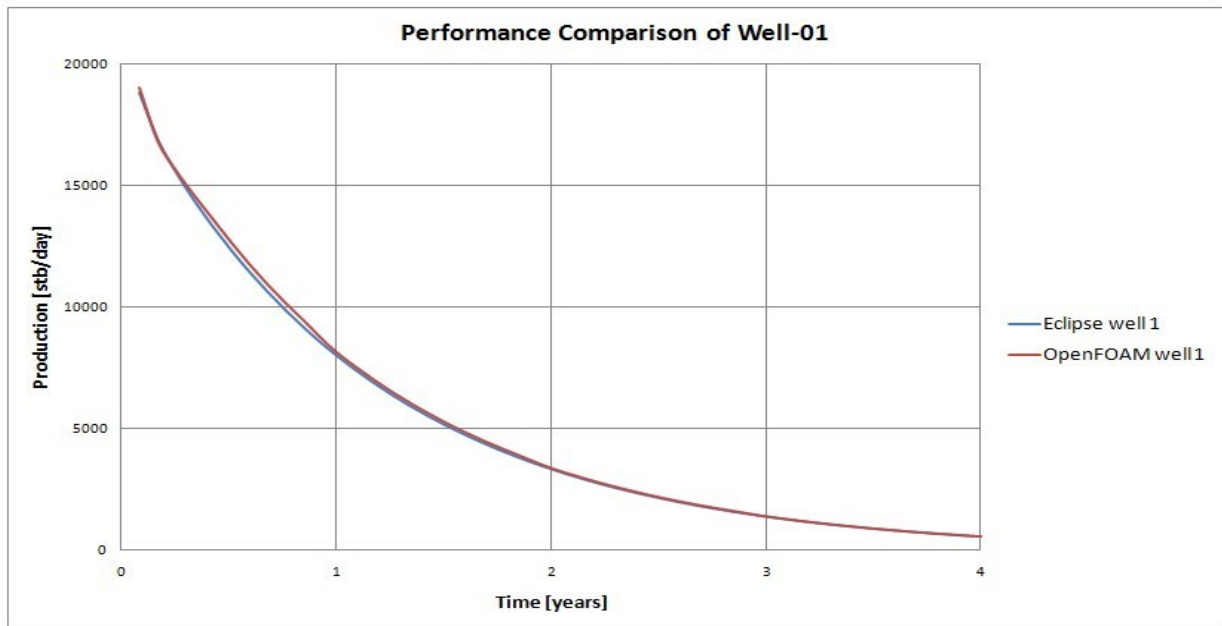
Figure 4-10:   Comparison of well 1 at constant BHP

Again, both simulation tools show similar production performance. A small discrepancy of the results can be observed in the beginning, between the 5th to 11th months.

The next plot shows the daily field production, which is the daily sum of all wells in field TESTCASE_1. A minimal discrepancy of approximately 300 STB/day can be observed in the period between 5 to 11 month. After 12 month both curves overlap well and the difference minimizes to less than 40 STB/day.
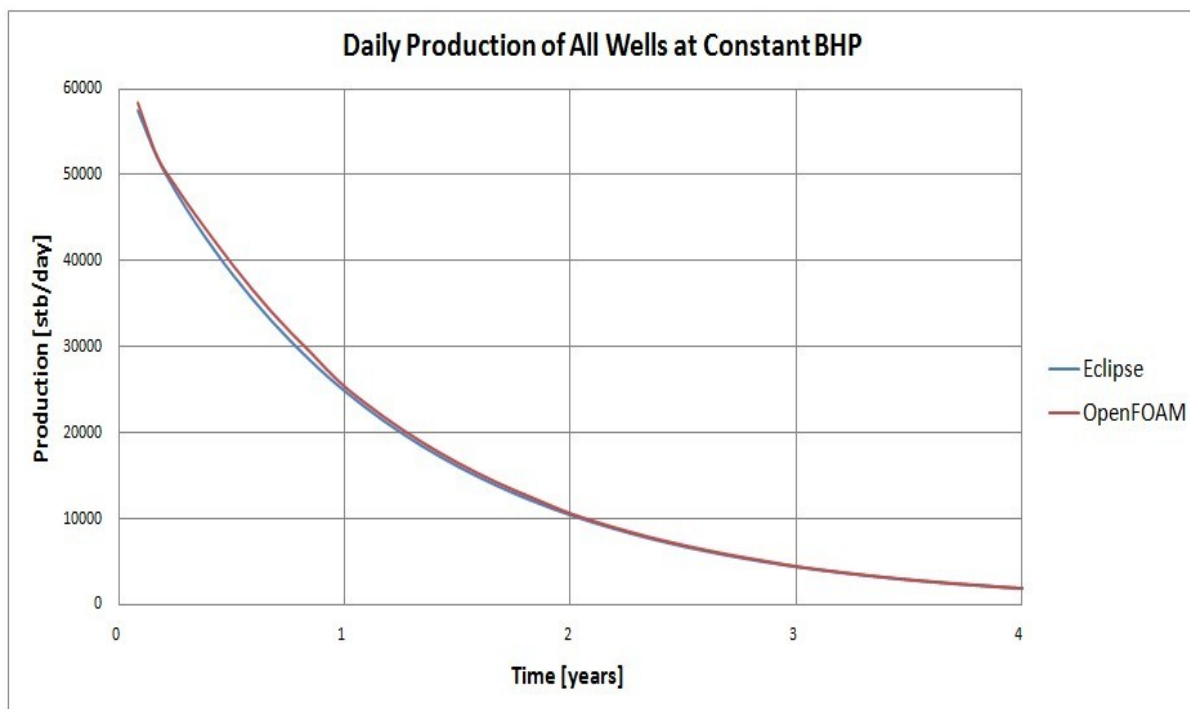
Figure 4-11:   Comparison of the daily field production

Figure 4-12 represents a cumulative production plot of the daily field production. This plot is a standard plot for reservoir engineers and gives an insight to the total production during the field life.
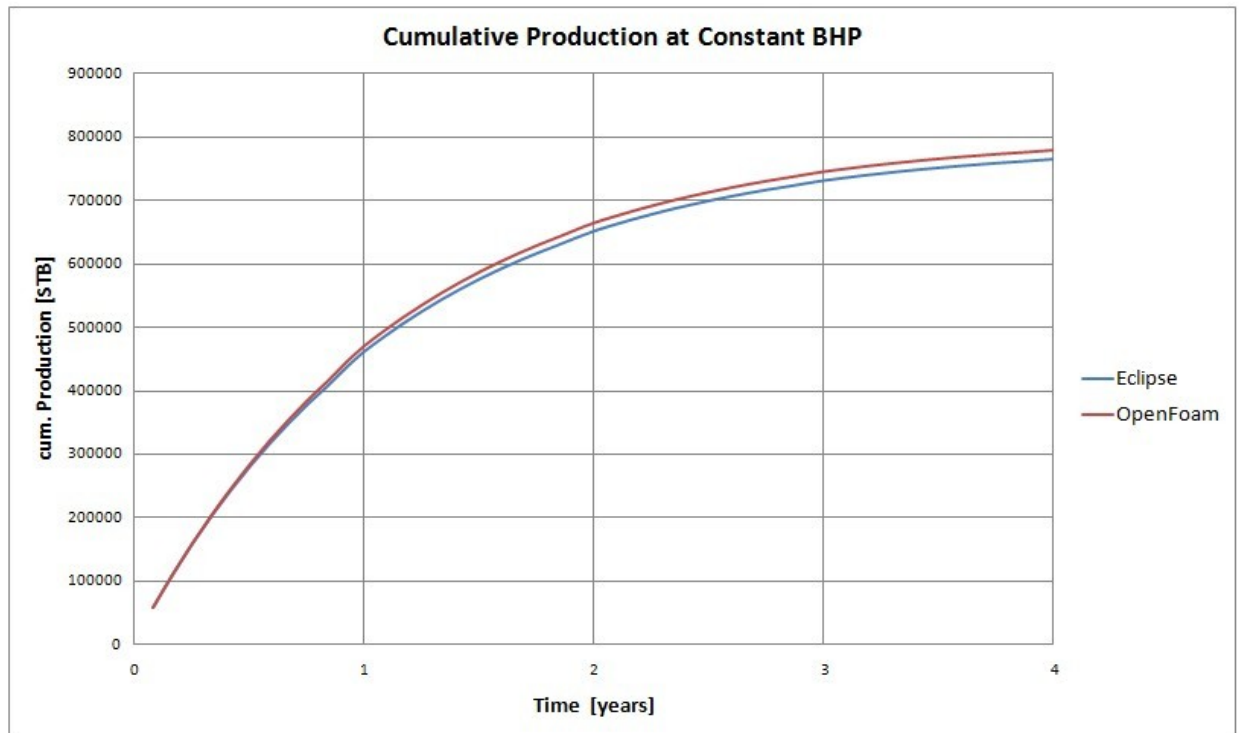
Figure 4-12:   Comparison of cumulative production

The observed higher daily production rate of OpenFOAM, which also can be reviewed in Table 4-4, leads to an increase in cumulative production. Eventually the difference between both forecasts amounts to a difference of 3.720 [STB] after four years, which represents just 1,48 % of the total production.

Finally, the results of TESTCASE_1 at constant BHP are shown in Table 5-4, focusing on the beginning and end time of simulation. The last two columns represent the daily sum of each time interval and the overall cumulative production of the whole field.

ECLIPSE performance in STB/day

Time [days]	Well 01	Well 02	Well 03	daily ∑	cum. Prod.
31	18850,49	19336,96	19315,11	57502,56	57502,56
62	16949,06	17578,09	17524,29	52051,44	109554,00
93	15594,06	16245,48	16162,84	48002,38	157556,38
124	14428,19	15063,29	14959,82	44451,29	202007,68
155	13374,73	13980,11	13863,96	41218,80	243226,47
186	12407,46	12978,59	12856,29	38242,34	281468,82
217	11514,12	12050,00	11926,25	35490,37	316959,19
248	10687,15	11188,30	11066,30	32941,75	349900,93
•	•	•	•	•	•
year 1	8069,71	8453,61	8351,37	24874,69	460318,03
•	•	•	•	•	•
year 2	3372,54	3533,73	3488,97	10395,23	651194,84
•	•	•	•	•	•
year 3	1414,87	1482,45	1463,65	4360,98	731132,76
•	•	•	•	•	•
1221	1054,79	1105,17	1091,18	3251,14	745700,31
1252	980,14	1026,95	1013,95	3021,04	748721,34
1283	910,77	954,27	942,19	2807,24	751528,58
1314	846,21	886,75	875,24	2608,20	754136,78
1345	786,31	823,88	813,41	2423,60	756560,38
1376	730,73	765,73	755,78	2252,24	758812,62
1407	679,23	711,72	702,42	2093,36	760905,99
1434	636,98	667,43	658,74	1963,16	762869,14
year 4	597,37	625,92	617,78	1841,07	764710,21

OpenFOAM performance in STB/day

| Time [days]	Well 01	Well 02	Well 03	daily ∑	cum. Prod.
31	19554,80	20191,40	20199,10	59945,30	58368,00
62	17308,70	18143,20	18117,10	53569,00	110529,90
93	16060,20	16942,50	16868,30	49871,00	159091,00
124	15015,70	15827,60	15708,90	46552,20	204420,20
155	14033,00	14772,80	14626,50	43432,30	246711,50
186	13054,40	13748,60	13588,90	40391,90	286042,20
217	12131,40	12783,40	12626,10	37540,90	322596,80
248	11268,40	11880,20	11730,30	34878,90	356559,20
•	•	•	•	•	•
year 1	8187,72	8634,37	8521,64	25343,73	470064,08
•	•	•	•	•	•
year 2	3402,94	3588,61	3541,81	10533,36	665170,80
•	•	•	•	•	•
year 3	1414,36	1491,53	1472,08	4377,97	746262,57
•	•	•	•	•	•
1221	1083,99	1143,13	1128,23	3355,35	760896,05
1252	1007,51	1062,48	1048,63	3118,62	763932,73
1283	936,43	987,52	974,65	2898,60	766755,17
1314	870,36	917,85	905,88	2694,10	769378,48
1345	808,96	853,10	841,97	2504,03	771816,71
1376	751,89	792,91	782,57	2327,36	774082,93
1407	698,84	736,97	727,36	2163,17	776189,26
1434	649,54	684,98	676,04	2010,55	778146,98
year 4	603,71	636,65	628,35	1868,70	779966,58

Table 4-4: ECLIPSE and OpenFOAM forecast at constant BHP

Table 4-4 once again illustrates, that there is no major difference between results of OpenFOAM and ECLIPSE at constant BHP.

4.1.2 TESTCASE_1 at Constant Production Rate

For this simulation scenario, the production rate of all wells is set to 100 [m³/day]. This restriction of production rate will lead to a roughly linear decline in BHP, since conditions are homogeneous and symmetric all across the reservoir and for both simulation tools. Once more the results for identical wells of OpenFOAM and ECLIPSE are compared. Well number 2 shows the highest deviation and is picked out for comparison reasons in Table 4-5. The percentage difference is as low as 0,07 % after the first year of production and rises to 1,35 % after 4 years.

Summary of TESTCASE_1 at constant production rate

Differences between OpenFOAM and ECLIPSE	Time-step	Well number:	[psi]	[%]
Max.result difference between OpenFoam and ECLIPSE	after 1 year	#2 ECLIPSE - #2 OpenFOAM	3,22	0,07
	after 4 years	#2 ECLIPSE - #2 OpenFOAM	46,91	1,35

Table 4-5: Comparison between OpenFOAM and ECLIPSE of TESTCASE_1 at constant production rate

The resulting low internal differences are again attributable to the homogeneous and symmetrical structure of the test case and wells conditions used in TESTCASE_1. This will lead to a similar performance of all six wells, analogical to TESTCASE_1 at constant BHP in chapter 4.1.1. Since all wells perform identically and overlap in a time versus pressure plot, it is less expressive to plot all six wells at once. Representative for the field performance, well number 1 is plotted for comparison between OpenFOAM and ECLIPSE in Figure 4-13.
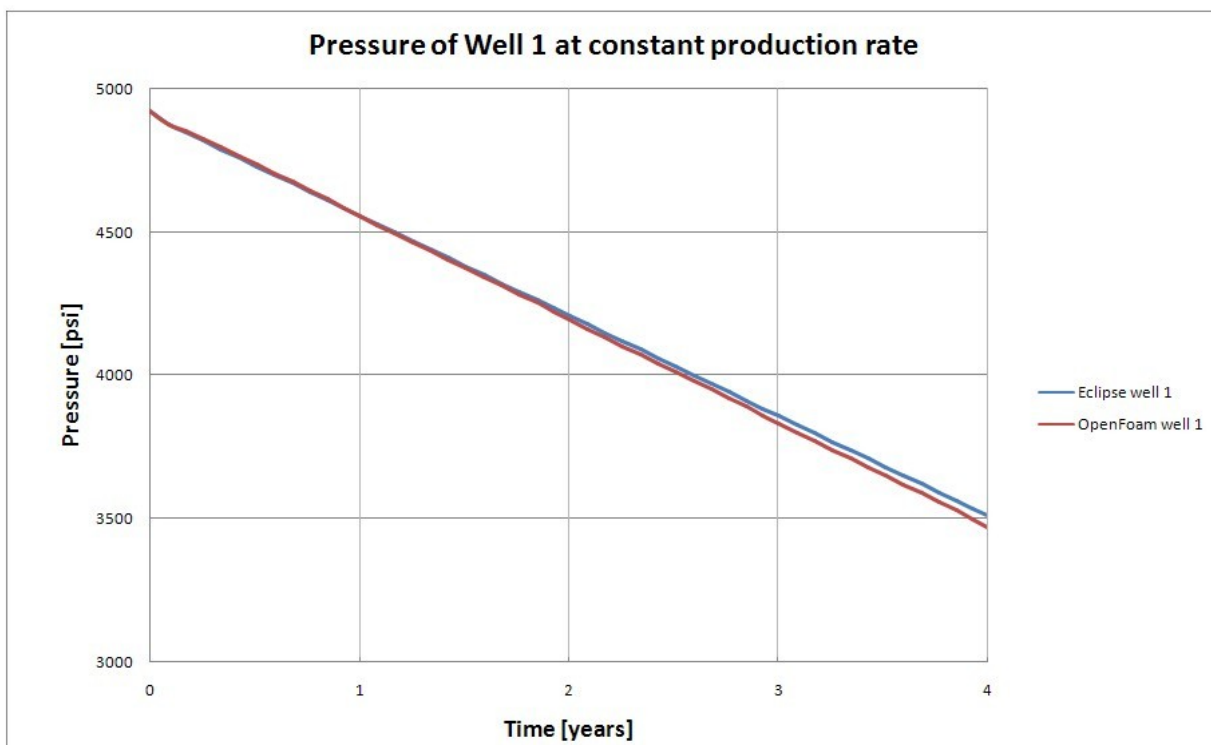
Figure 4-13: Pressure of well 1, at constant production rate

After production has started, the BHP decreases linearly. As external boundaries are closed, isolating the reservoir, there is no external driving-force acting on the reservoir pressure to reduce the pressure decline. The force to drain this reservoir is only based on the initial pore pressure and the rock compressibility leading to a depletion of the reservoir. This decline rate of pressure certainly depends on applied production rates, phase viscosity rock compressibility and permeability. Again, the comparison shows a similar performance during the whole simulation on a pressure versus time plot.

In Table 4-6 pressure data of TESTCASE_1 for all three wells at constant production rate, in respect of OpenFOAM and ECLIPSE, can be seen.

ECLIPSE performance in psi				OpenFOAM performance in psi			
Time [days]	Well 01	Well 02	Well 03	Time [days]	Well 01	Well 02	Well 03
0	4920,75	4920,75	4920,75	0	4920,75	4920,75	4920,75
31	4877,50	4878,93	4878,68	31	4873,95	4874,02	4874,00
62	4847,39	4849,00	4848,57	62	4850,61	4853,35	4851,99
93	4818,39	4819,83	4819,62	93	4823,85	4825,90	4825,18
124	4788,26	4789,92	4789,40	124	4794,81	4796,71	4796,41
155	4758,65	4760,18	4759,86	155	4765,09	4767,01	4766,62
186	4728,69	4730,36	4729,82	186	4735,23	4737,03	4736,63
217	4699,30	4700,80	4700,54	217	4704,93	4706,79	4706,44
•	•	•	•	•	•	•	•
year 1	4557,73	4559,39	4558,86	year 1	4554,26	4556,17	4555,82
•	•	•	•	•	•	•	•
year 2	4207,46	4209,20	4208,51	year 2	4192,45	4194,31	4193,92
•	•	•	•	•	•	•	•
year 3	3857,58	3859,21	3858,72	year 3	3830,64	3832,60	3832,21
•	•	•	•	•	•	•	•
1221	3739,09	3740,68	3740,28	1221	3710,16	3711,96	3711,61
1252	3708,99	3710,56	3710,22	1252	3680,05	3681,87	3681,47
1283	3679,70	3681,30	3680,88	1283	3649,93	3651,69	3651,32
1314	3649,93	3651,52	3651,13	1314	3619,75	3621,59	3621,20
1345	3620,67	3622,26	3621,86	1345	3589,46	3591,40	3591,03
1376	3590,70	3592,29	3591,90	1376	3559,50	3561,28	3560,92
1407	3561,05	3562,64	3562,24	1407	3529,24	3531,08	3530,69
1434	3535,09	3536,69	3536,29	1434	3499,04	3500,96	3500,56
year 4	3509,86	3511,45	3511,04	year 4	3469,52	3464,54	3464,02

Table 4-6: ECLIPSE & OpenFOAM forecast at constant production rate

As mentioned before, Table 4-6 once again illustrates, that there is no major difference between results of OpenFOAM and ECLIPSE.

4.1.3 Streamlines of the flow field in TESTCASE_1

The velocity-data-files from our test-case can be used by ParaView to create streamlines of the flow field in the reservoir. In general, the fluid flow within a continuum is characterized by a velocity vector field. By drawing tangents to the velocity vector of the flow field, a number of streamlines will be obtained. These streamlines show the direction a fluid element will travel at any point in time. The resulting picture of such stream-tracer function can be seen in Figure 4-14.
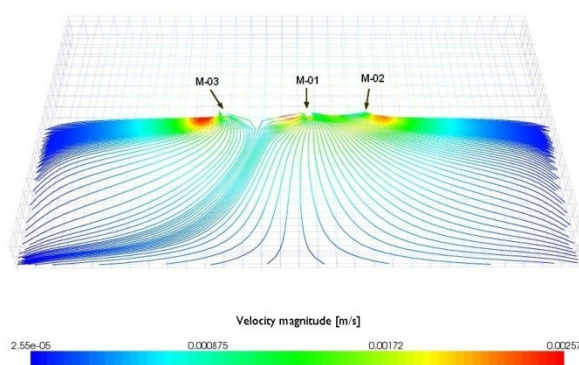
Figure 4-14:   Streamlines of TESTCASE_1 in horizontal view

A detailed picture of the flow near the wellbore can be seen in Figure 4-15.
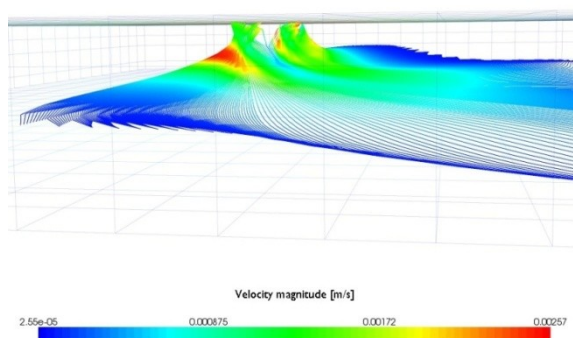
Figure 4-15: Streamlines near the wellbore of TESTCASE_1

This detailed visualization of velocity magnitude is helpful to illustrate flow schemes around the perforated well, as well as flow-filed characteristics inside the reservoir.

4.2 TESTCASE_2: Modified Common Reservoir

The results of TESTCASE_1 set the cornerstone for a more complex reservoir. The simplicity of the first test case - be it the symmetric well location, the homogeneous reservoir or the geometry - was ideal to gather experience and optimize simulation workflow.

It is obvious, that the next test case should provide a more complex, more sophisticated structure, based on "real" reservoir geometry in order to show possible limitations of OpenFOAMs PRSFoam solver. The case study TESTCASE_2 represents a simplified, fictive oil reservoir, such as slightly compressible rock and incompressible fluid, but is based on realistic seismic data.

DI. Dr. Georg Mittermeier, reservoir engineer of HOL GmbH, modified a common inhomogeneous reservoir, based on a real data set into an appropriate test case. These efforts led to the creation of MODEL_TESTCASE_2_IFR_E100, short: TESTCASE_2. It was further modified and converted to meet the requirements of a professional comparison between ECLIPSE and OpenFOAM. The structure of TESTCASE_2 can be seen in Figure 4-16.
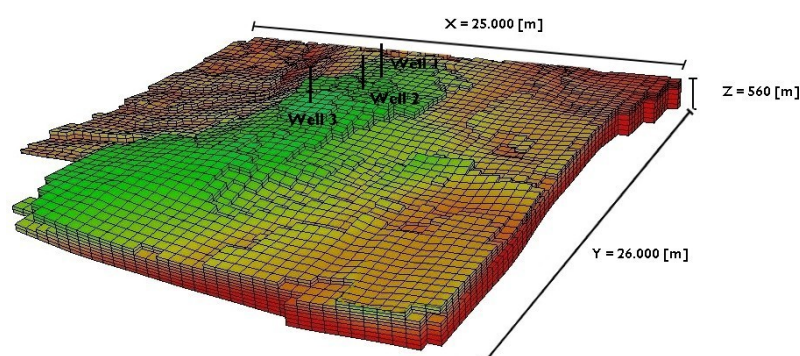
Figure 4-16:   Dimensions of TESTCASE_2

The reservoir is vertically divided into fourteen layers and consists of a higher permeable flow-path in the center of the reservoir and a low permeable rock structure close to outer boundaries. The reservoir is again bounded by no flow walls on all six sides and appears to be closed for external driving forces. Three production wells are defined, which are located in the northern part of the reservoir. This can be seen in Figure 4-16.

The next paragraph briefly introduces facts and dimensions of TESTCASE_2:

The size of case TESTCASE_2 is 25.000 [m] in y direction, times 26.000 [m] in x direction and times 560 [m] in vertical z direction. These dimension results in a total reservoir volume of 3,64E+11 [m³]. The OOIP of field TESTCASE_2 is harder to evaluate before simulation due to the inhomogeneity of the reservoir. TESTCASE_2 consist of a block sum (50 x 52 x 14) of 36.400. The Cartesian grid is composed of blocks with the size 500 [m], times 500 [m], times 40 [m]. This leads to a total volume of 10E+6 [m³] per block.

The simulation was increased to 20 years and time steps were set to 3 days. All additional details of the geometry and static properties are listed in Table 4-7.

	Variables	Description	Values	Units
general properties:	TVD	reference depth	4.000	[m]
	t	simulated production time	20	[years]
	Δt	time interval of simulation steps	3	[days]
	Δt_{wr}	file writing interval	3	[days]
	K(z)	grid blocks in z direction	14	[blocks]
	I(x)	grid blocks in x direction	50	[blocks]
	J(y)	grid blocks in y direction	52	[blocks]
	$\sum$ grids	total sum of blocks	36.400	[blocks]
transport properties:	μ	average viscosity	0,01	[m²/s]
	p_{init}	pressure @ reference depth	200	[bar]
rock properties:	ρ	fluid density	883,65	[kg/m³]
	Φ	rock porosity	up to 18	[%]
well properties:	$\sum$ well	total number of wells	3	
	r_w	well radius	0,155448	[m]

Table 4-7: Input parameter for TESTCASE_2

Similar to TESTCASE_1, two production scenarios are performed. First, all wells produce at a constant rate of 100 [m³/day] and pressure data is recorded. The second scenario

simulates a BHP limitation of 50 [bar] for all three wells, where the corresponding production rate is logged.

According to the input data, the simulation of TESTCASE_2 is launched at both simulation tools, ECLIPSE and OpenFOAM. In Table 4-8 the comparison between ECLIPSE and OpenFOAM's wall-clock-time and the required memory is listed.

Comparison of simulation time and required memory		
Processor: Intel Core2 Duo CPU P8400 @ 2.26GHz System: 32Bit operating system		
TESTCASE_2		
	ECLIPSE_100	PRSFoam
Wall clock time: [s]	121	187
Required memory: [MB]	23,94	35,22

Table 4-8: TESTCASE_2: Computational simulation comparison

PRSFoam, which was faster in the simplified TESTCASE_1, presently necessitated more time and memory for the more complex TESTCASE_2.

4.2.1 TESTCASE_2 at Constant Production Rate

The first simulation scenario is calculated at a constant production rate of 100 [m³/day], which is applied to each single well. The resulting pressure forecast is approximately identical with the results of a constant BHP production scenario, hence resulting in analogous post-processing screenshots. Therefore, only the pressure distribution results of the constant production rate scenario are imaged in this chapter. Common hydrocarbon reservoirs exhibit high horizontal latitude – up to 100 kilometers. Yet in most cases the vertical dimension shows only a few meters in reservoir height because of geological and geophysical reasons. Due to this fact, for post-processing purposes, the height of the

reservoir is extended four times to improve visualization of the pressure distribution within the reservoir layers.

Figure 4-17 and Figure 4-18 show the result of ECLIPSE and OpenFOAM for TESTCASE_2 after 1 [year] of constant production.
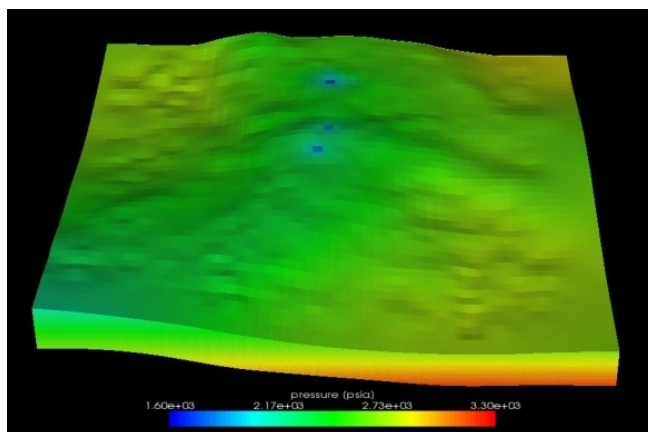
Figure 4-17:   ECLIPSE results of pressure distribution after one year of production
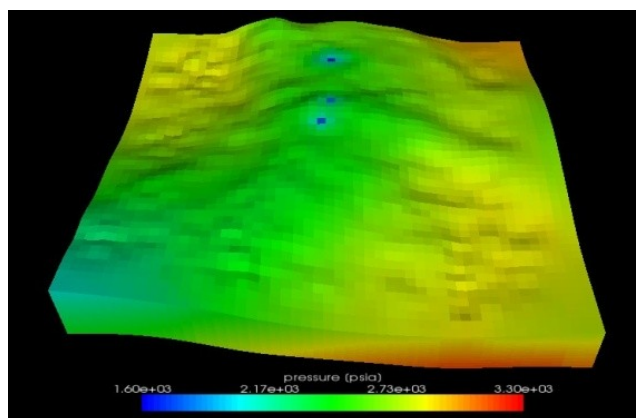
Figure 4-18:   OpenFOAM results of pressure distribution after one year of production

A difference to be noted is the tendency of ECLIPSE to establish "pressure layers" in low permeable regions, while OpenFOAM results in a high pressure "hot-spot" in these low permeable areas, which can be recognized in both screenshots in Figure 4-17/4-18 and upcoming Figure 4-19/4-20. The reservoir is drained by three wells, lowering the pressure

faster in high permeable regions. All three wells are characterized by a blue, low-pressure production block. As one can see, red areas retain a higher pressure, due to the fact that fluid expands slower within the low permeable region and conveys the impression of pressure accumulation. Vice versa, green areas of lower pressure and high permeability facilitate the transfer of fluid, therefore pressure differences distribute faster between neighboring blocks.

After 20 years of oil production, the simulation was stopped. The final pressure distribution of ECLIPSE and OpenFOAM simulation is shown in Figure 4-19 and Figure 4-20.
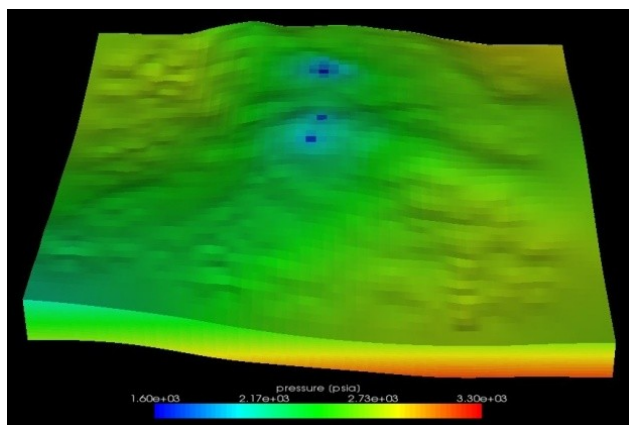
Figure 4-19:   ECLIPSE result after 20 years of production
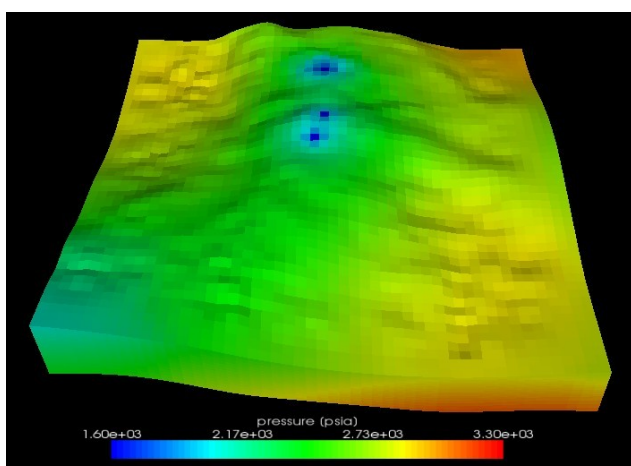
Figure 4-20:   OpenFOAM result after 20 years of production

Once again, both solvers show similar pressure distribution results after 20 years of production.

Figure 4-21 shows the field performance of TESTCASE_2, comparing both simulation tools. The dotted OpenFOAM curves fall with a faster rate and have a higher pressure at the simulation start.
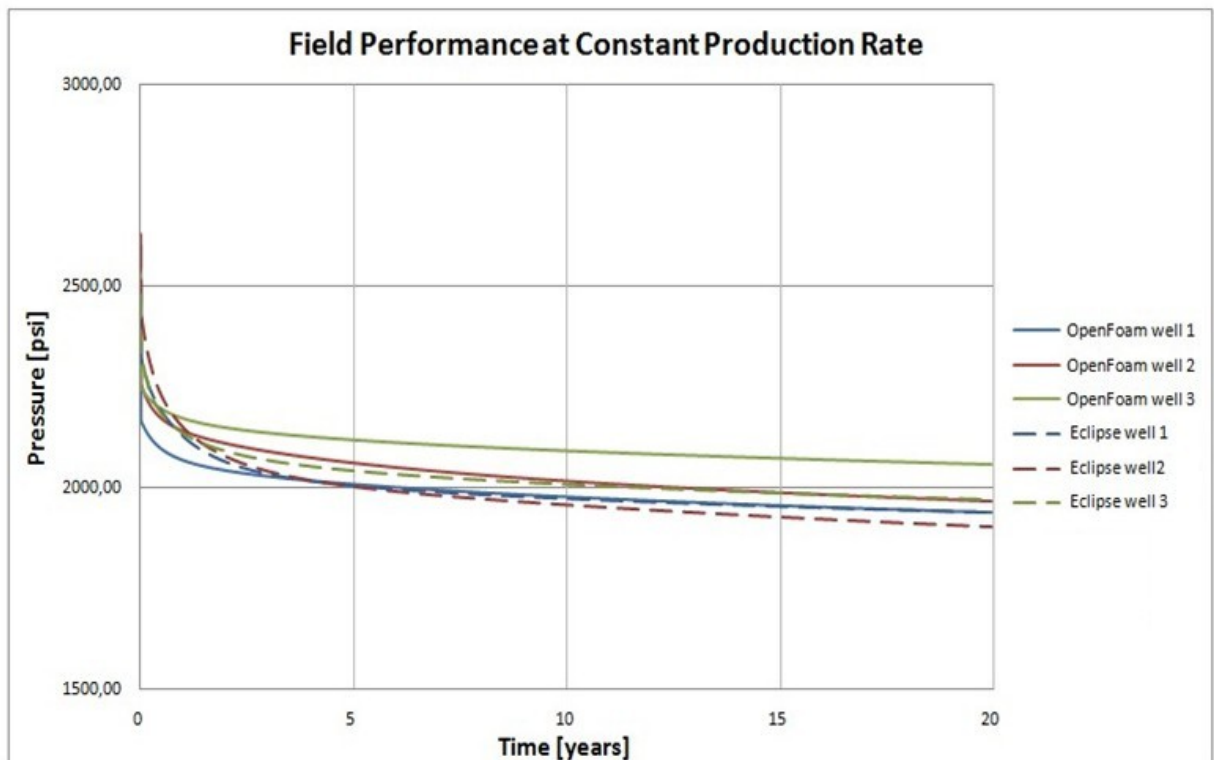
Figure 4-21: TESTCASE_2 field performance at constant production rate

All wells show the similar BHP decline after 5 years of production. A major difference can be observed for the wells to change from a transient behavior onto a constant linear decline at the beginning of the constant production. OpenFOAM pressure results are a little lower than its ECLIPSE counterparts after 20 years of constant production. The maximum difference at well 3 is slightly above 4,4 %, which can be seen in Table 4-9.

OpenFOAM also calculates a shorter transient time for all wells during the first two years. More differences between OpenFOAM and ECLIPSE forecasts can be seen in Table 4-9.

Summary of TESTCASE_2 at constant production

Differences between OpenFOAM and ECLIPSE	time-step	well number:	value [psi]	[%]
max.result difference between OpenFoam and ECLIPSE	after 1 year	#1 OpenFOAM - ECLIPSE	59,88	2,81
		#2 OpenFOAM - ECLIPSE	8,09	0,38
		#3 ECLIPSE - OpenFOAM	36,91	1,73
	after 10 years	#1 ECLIPSE - OpenFOAM	5,11	0,26
		#2 ECLIPSE - OpenFOAM	61,00	3,12
		#3 ECLIPSE - OpenFOAM	83,92	4,18
	after 20 years	#1 OpenFOAM - ECLIPSE	0,84	0,04
		#2 OpenFOAM - ECLIPSE	65,67	3,45
		#3 OpenFOAM - ECLIPSE	88,00	4,47

Table 4-9: Differences of TESTCASE_2 at constant production

As one can see, the differences between ECLIPSE and OpenFOAM are in general between 0,04 % and 4,47 % after 20 years of production. This maximum in differences is relatively small for a complex reservoir, such as TESTCASE_2.

To enable a better comparison, well number 2 and 3 were selected and plotted in Figure 4-22. OpenFOAM performances of both wells are colored blue, while ECLIPSE performance is colored red.
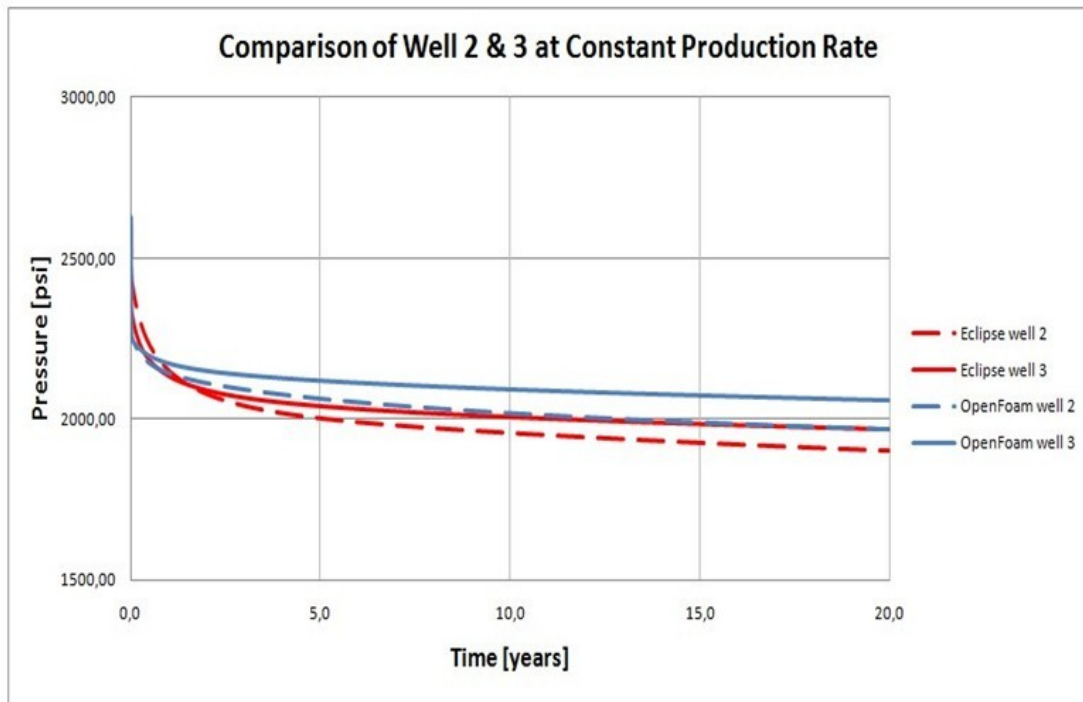
Figure 4-22: Comparison of well 2 and 3 at constant production rate

ECLIPSE well number 3 needs a rather short transient time to reach a constant linear decline, while well number 2 requires more than three years transient time. Finally both simulation tools are in accordance with each other, as they show that well number 2 and well number 3 slowly drift apart between three and seven years and finally perform in a similar decline as production time goes on.

The recorded pressure data of TESTCASE_2 at constant production rate are listed below in Table 4-10.

Eclipse performance in psi

Time [days]	Well 01	Well 02	Well 03
0	2452,26	2602,54	2477,90
3	2323,85	2436,35	2339,13
6	2319,59	2429,50	2332,94
9	2315,46	2422,85	2327,01
12	2311,47	2416,39	2321,33
15	2307,60	2410,12	2315,88
18	2303,85	2404,04	2310,65
21	2300,21	2398,14	2305,64
•	•	•	•
year 1	2128,95	2151,50	2135,73
•	•	•	•
year 5	2004,85	2003,48	2041,74
•	•	•	•
year 10	1972,52	1958,06	2007,80
•	•	•	•
year 15	1952,99	1927,69	1986,27
•	•	•	•
7270	1938,07	1903,53	1969,86
7273	1938,05	1903,49	1969,83
7276	1938,02	1903,45	1969,81
7280	1938,00	1903,41	1969,78
7283	1937,98	1903,37	1969,76
7286	1937,95	1903,34	1969,73
year 20	1937,93	1903,30	1969,71

Openfoam performance in psi

Time [days]	Well 01	Well 02	Well 03
0	2522,27	2628,84	2528,77
3	2169,90	2261,33	2252,15
6	2165,49	2257,34	2247,57
9	2163,37	2254,49	2246,13
12	2161,29	2251,72	2244,69
15	2159,26	2249,04	2243,29
18	2157,29	2246,45	2241,91
21	2155,36	2243,93	2240,56
•	•	•	•
year 1	2069,07	2143,41	2172,64
•	•	•	•
year 5	2009,12	2064,02	2118,83
•	•	•	•
year 10	1977,63	2019,06	2091,72
•	•	•	•
year 15	1955,86	1990,26	2072,94
•	•	•	•
7270	1938,93	1969,16	2057,86
7273	1938,90	1969,13	2057,83
7276	1938,88	1969,10	2057,81
7280	1938,85	1969,06	2057,78
7283	1938,82	1969,03	2057,76
7286	1938,80	1969,00	2057,73
year 20	1938,77	1968,97	2057,71

Table 4-10: ECLIPSE & OpenFOAM forecast at constant production rate

One important observation can be made at the initial time step in Table 4-10. The difference of the unequal depths of the perforated blocks is the reason for the spread in overburden pressure between wells of the same simulation tool. Wells of the same number (1, 2 or 3) should start at a similar pressure level. However, the initial well pressures differ by approximately 4,7 % between same wells of ECLIPSE and OpenFOAM.

Each well starts at different heights, relative to the surface. The initial pressure is calculated according to the of gravity equilibrium conditions [4] in chapter 2.7.1. It could be, that ECLIPSE and OpenFOAM calculate and interpolate these values according to different mathematical standards.

["

In Figure 4-23 the field production according to the applied BHP is plotted. The dashed lines represent the results of the OpenFOAM solver. Full lines, drawn in same well color, illustrate the results of Schlumberger's ECLIPSE_100 solver.

Both ECLIPSE and OpenFOAM show a similar performance. Further on, well 3 is in both programs an outlier. In contrast to results of the constant production rate, where all three wells produce similarly at a constant pressure, well number 3 exhibits the ability to produce at higher rates, than well number 1 and 2. Well number 3 is set in an area of higher permeability. It is a very positive finding that both ECLIPSE and OpenFOAM show a concordance of higher production rate for well number 3. But next to the higher rate, well number 3 also exhibits a linear relationship similar to well 1 and 2 after three years.

The most significant graph for TESTCASE_2 is presented in Figure 4-23.
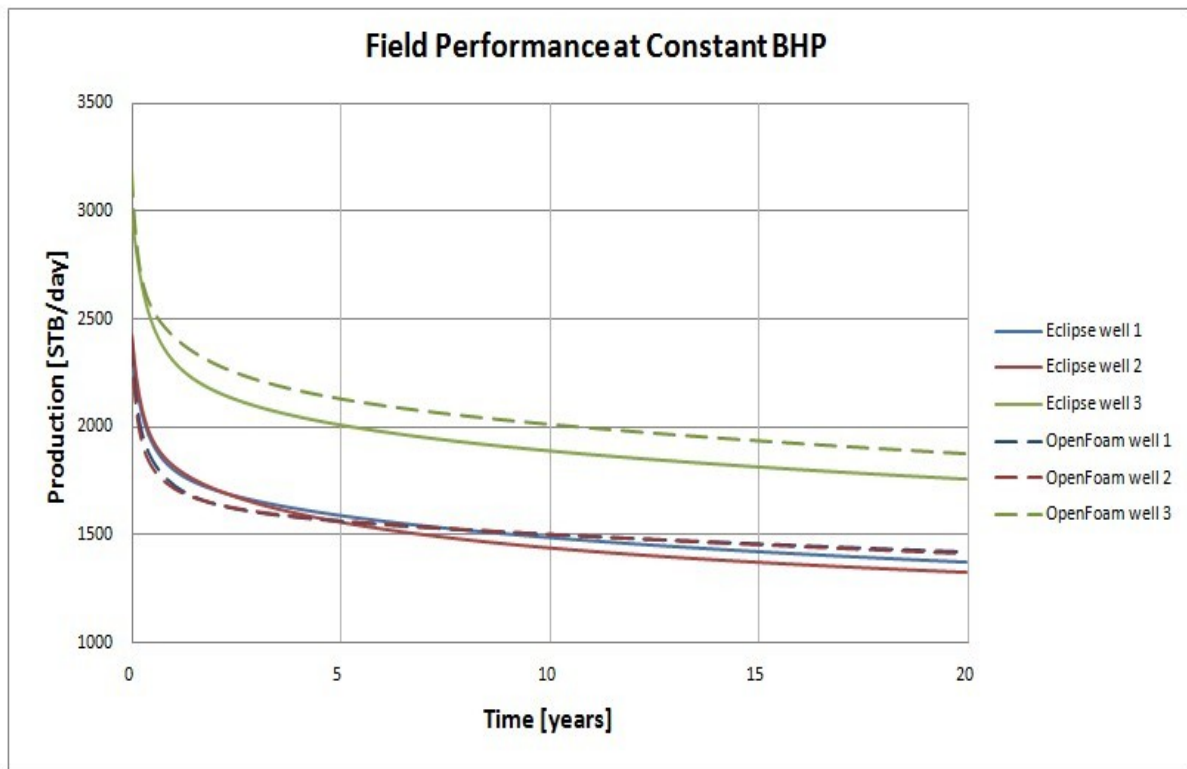
Figure 4-23: TESTCASE_2 complete field performance at constant BHP

After 20 years, the difference between well number 2 and well number 3 amounts to:

- 432 STB/day according to ECLIPSE forecast

- 461 STB/day according to OpenFOAM forecast

This represents a difference of 29,00 STB/day, or 6,29 %, which is similar to differences in constant production calculation of TESTCASE_2 in chapter 4.2.1 .

The results for the field performance of Testcase_2 are satisfying, since both simulation tools predict a significant higher performance of well number 3. The production of well number 3 differs roughly by 100 STB/day between OpenFOAM and ECLIPSE.

However, this graph has already convincingly demonstrated that both tools use identical reservoir structures, perform under similar production models and thus result in analogue production and pressure forecasts.

After summing up the daily production for all combined wells, both graphs are compared in Figure 4-24. The comparison of both simulation results shows a related rate decline. Disparities in production fall to a level less than 255 STB/day.
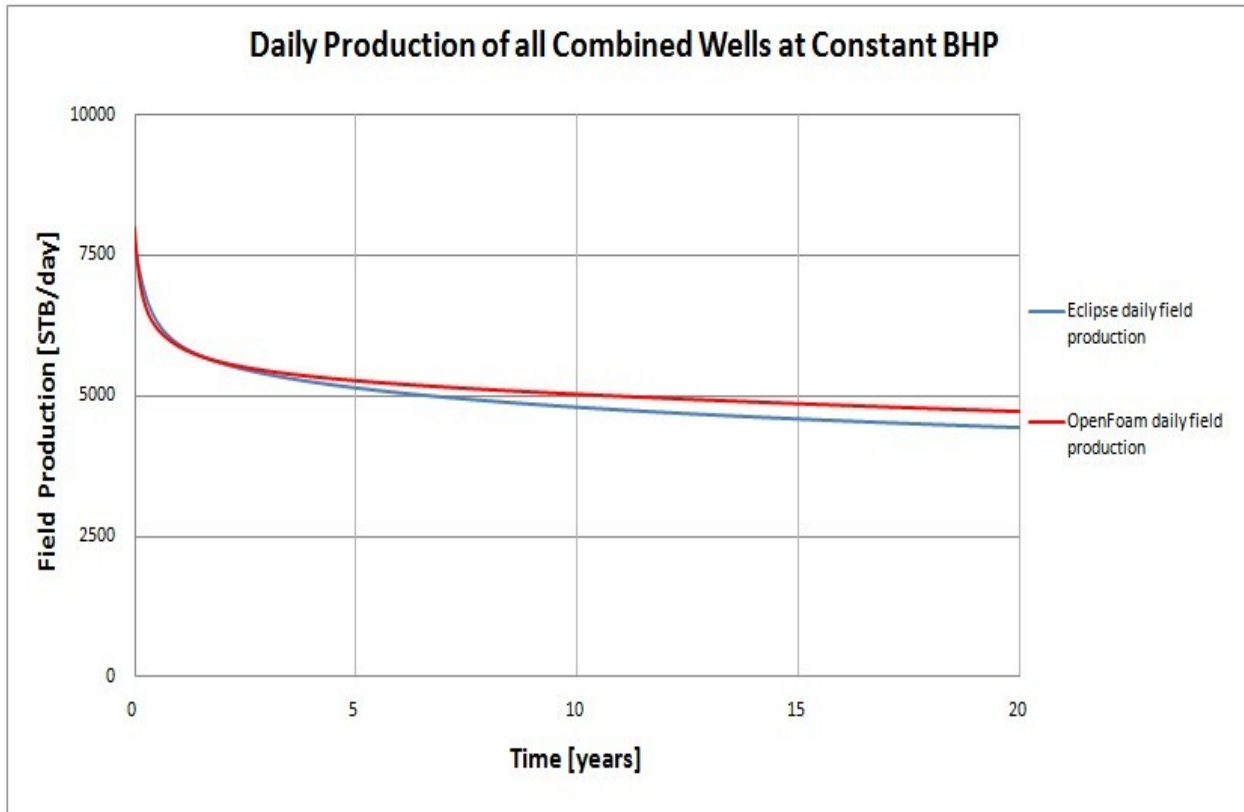
Figure 4-24:   Comparison of the daily field production

Another significant factor to classify the performance of a reservoir is the recorded cumulative production. This evaluation method can be used to compare the quality of ECLIPSE and OpenFOAM results. The corresponding graph is seen in Figure 4-25.

After 20 years of simulation the difference in cumulative production is 3,78E+5 barrels, or 3,14 %.
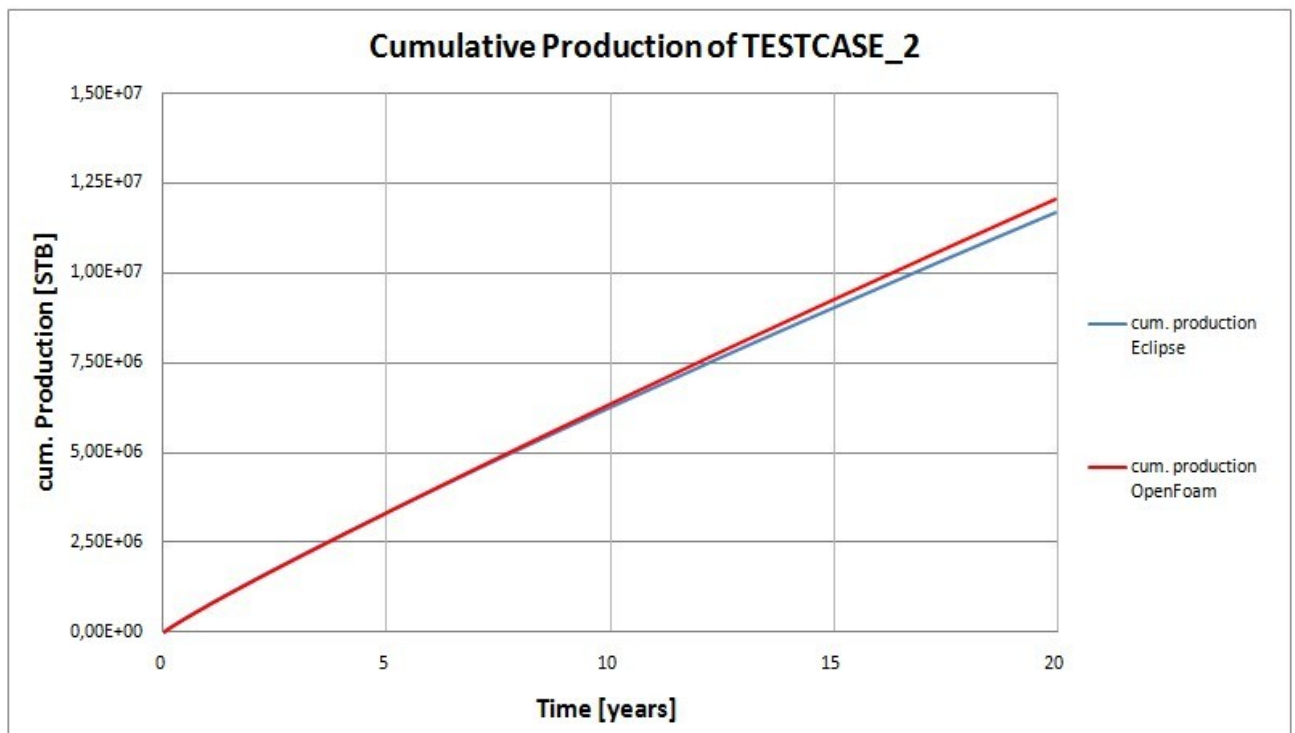
Figure 4-25:   Comparison of the ultimate cumulative production

Finally, Table 4-12 visualizes all results of ECLIPSE and OpenFOAM simulation at constant BHP. However, it has to be kept in mind that this comparison represents an idealized case, where fluid properties and flow conditions are chosen to meet OpenFOAM requirements.

Eclipse performance in STB/day

Time [days]	Well 01	Well 02	Well 03	daily Σ	cum. Prod.
3	2327,93	2422,71	2966,04	7716,68	7716,68
6	2329,94	2417,62	2970,87	7718,43	15435,11
9	2315,61	2398,44	2954,96	7669,01	23104,12
12	2301,67	2379,96	2939,36	7620,99	30725,11
15	2288,18	2362,23	2924,18	7574,59	38299,69
18	2275,14	2345,19	2909,40	7529,74	45829,43
21	2262,52	2328,83	2895,03	7486,37	53315,80
24	2250,30	2313,10	2881,03	7444,43	60760,23
•	•	•	•	•	•
year 1	1804,86	1817,51	2303,06	5925,43	765196,8525
•	•	•	•	•	•
year 5	1591,52	1555,43	2005,52	5152,47	3335233,925
•	•	•	•	•	•
year 10	1489,65	1435,92	1885,15	4810,73	6263542,393
•	•	•	•	•	•
year 15	1424,40	1368,93	1810,49	4603,82	9036935,36
•	•	•	•	•	•
7270	1376,62	1323,21	1754,69	4454,52	11652977,12
7273	1376,55	1323,15	1754,60	4454,29	11657431,42
7276	1376,47	1323,08	1754,51	4454,06	11661885,48
7280	1376,40	1323,01	1754,43	4453,83	11666339,31
7283	1376,33	1322,94	1754,34	4453,60	11670792,91
7286	1376,25	1322,87	1754,25	4453,37	11675246,28
year 20	1376,18	1322,80	1754,16	4453,14	11679699,43

Openfoam performance in STB/day

| Time [days]	Well 01	Well 02	Well 03	daily Σ	cum. Prod.
3	2401,67	2393,08	3179,09	7973,84	7973,84
6	2367,44	2348,88	3144,10	7860,42	15834,26
9	2336,27	2310,42	3111,41	7758,10	23592,36
12	2307,94	2276,97	3080,91	7665,82	31258,18
15	2282,08	2247,52	3052,40	7582,00	38840,18
18	2258,36	2221,18	3025,67	7505,21	46345,39
21	2236,46	2197,28	3000,55	7434,29	53779,68
24	2216,17	2175,38	2976,90	7368,45	61148,13
•	•	•	•	•	•
year 1	1734,84	1717,54	2419,14	5871,52	751515,66
•	•	•	•	•	•
year 5	1564,42	1564,58	2128,01	5257,01	3337735,67
•	•	•	•	•	•
year 10	1503,95	1501,91	2009,58	5015,44	6361515,28
•	•	•	•	•	•
year 15	1460,13	1454,10	1933,08	4847,31	9269050,77
•	•	•	•	•	•
7270	1423,17	1412,98	1873,85	4710,00	12030086,95
7273	1423,11	1412,91	1873,76	4709,78	12034796,73
7276	1423,05	1412,84	1873,66	4709,55	12039506,28
7280	1422,99	1412,78	1873,57	4709,34	12044215,62
7283	1422,93	1412,71	1873,48	4709,12	12048924,74
7286	1422,87	1412,64	1873,38	4708,89	12053633,63
year 20	1422,81	1412,57	1873,29	4708,67	12058342,30

Table 4-12:   ECLIPSE & OpenFOAM forecast at constant BHP

Comparing the results of both programs, the production per day differs by 3,88 % for well number 1, by 5,50 % for well number 2 and by 5,04 % for well number 3 after one year. These values change to 3,39 % for well number 1 and 6,79 % for well number 2 and 3 after 20 years of production.

The relative differences in production rate are indeed higher than the relative differences in pressure obtained from the constant production scenario.

One explanation for this behavior could be that ECLIPSE_100 just allows determining the Formation Volume Factor (FVF) close to 1 (see Table 4-13). This means that ECLIPSE_100 specifies the oil always as "slightly compressible"; while on the other hand, PRSFoam solver regards the oil always as totally incompressible.

PVT Keywords		PVDO (Dead Oil PVT Properties (No Dissolved Gas))		✓ ECHO
Dead Oil PVT Properties (No Dissolved Gas)		Echo Data Input		
Fluid Densities at Surface Conditions				

Row	Press (bar)	FVF (rm3 /sm3)	Visc (cp)	+
1	25	1	1.14	
2	50	0.99	1.14	
3	75	0.98	1.14	
4	100	0.97	1.14	
5	125	0.96	1.14	
6	150	0.95	1.14	
7	175	0.94	1.14	
8				
9				
10				
11				
12				

Apply   Reset   Help

Table 4-13: Pressure dependency of the Formation Volume Factor in ECLIPSE

Additional to the pressure dependency of the Formation Volume Factor, one can see that in row tree of Table 4-13 the viscosity remains constant with increasing pressure.

4.2.3   Streamlines of the flow field in TESTCASE_2

Again, the velocity-data-files of OpenFOAM can be used by ParaView to create a streamline plot of the flow field in the reservoir. The resulting streamlines through the center of the reservoir can be seen in Figure 4-26.
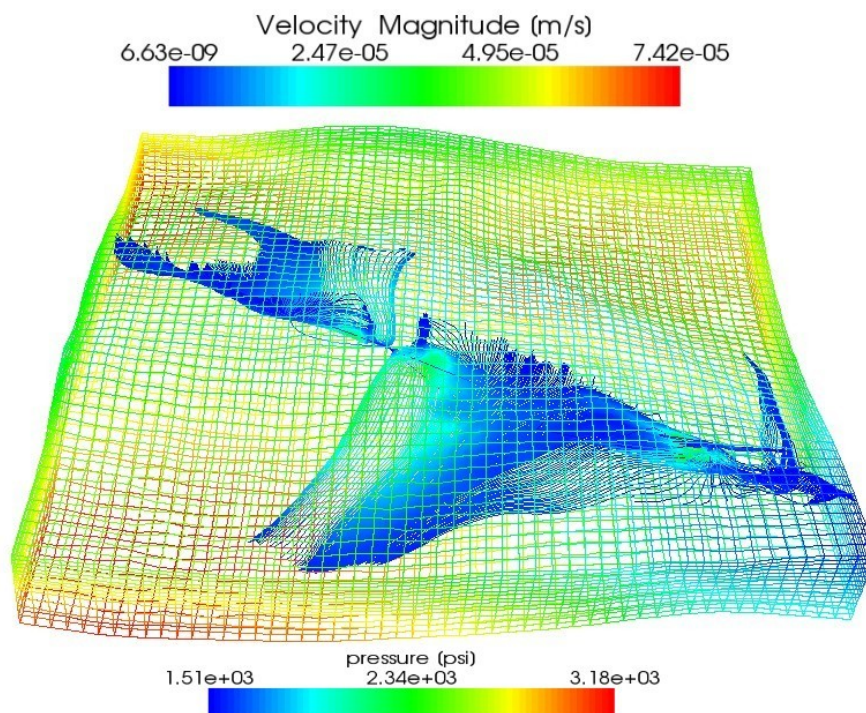
Figure 4-26:   Streamlines within the pressure mesh of TESTCASE_2

The streamlines are illustrated within the original reservoir geometry of TESTCASE_2. The pressure-distribution and the velocity magnitude are enlarged eight times to improve the visualization. For a better visualization, the height of the reservoir is extended six times.

In the next Figure 4-27, the line source penetrates the reservoir from the north to the south. The reservoir frame in the background reflects the permeability distribution in the x-direction of the bottom-layer.
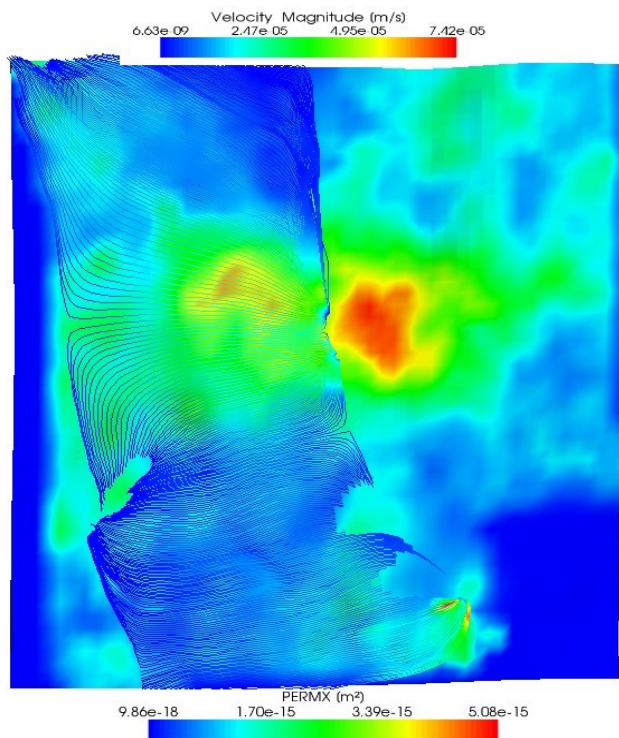
Figure 4-27:   Velocity streamlines compared to permeable structure of TESTCASE_2

To emphasize the structure of the drained reservoir, Figure 4-27 shows the corresponding streamlines in front of the permeability distribution of the bottom of TESTCASE_2. Again, the line-source is placed next to all three wells. As one can see, high permeable areas direct the velocity stream into the direction of the least resistance and highest conductivity. This can be seen at the right bottom of Figure 4-27 and at the centered left and around the permeable spot at the bottom.

4.3 WATER_INJECTION: Single-Phase Injection and Production Scenario

The third test-case represents a fictive injection-production scenario, where the initial reservoir fluid is displaced by an injection fluid of same density. PRSFoam is designed to process a single-phase displacement: this fact is disadvantageous when simulating an injection-production scenario. Hence, the displaced fluid has to have the same density as the injected fluid. This leads to an uncommon water–water displacement scenario to meet requirements of PRSFoam. However, the compositional solver of ECLIPSE processes this injection-production scenario and even results in a similar performance compared to OpenFOAM. The difference between both tools results from the fact that ECLIPSE_300 is not able to displace a phase using a phase of equal density. This will lead to an undefined displacement process and unspecific mixture of both, the injected and the produced fluid within the reservoir. Therefore the density value of the injected fluid was raised minimally for the simulation of the ECLIPSE case.

The reservoir is related to TESTCASE_1: a simple structured shoebox model exhibiting a single porosity - single permeable zone, which is penetrated by an injector well "I1" and one producer "P1".

A schematic illustration of test case WATER_INJECTION can be seen in Figure 4-28.
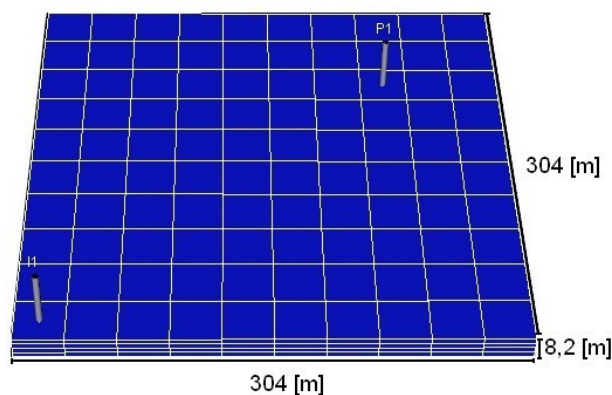
Figure 4-28:   Structure of test case WATER_INJECTION

The size of case WATER_INJECTION is defined by the following dimensions:

304 [m] in horizontal Y direction, 304 [m] In X direction and 8,20 [m] in vertical Z direction. These dimensions result in a total volume of 7,58E+5 [m³] and the "original water in place" of field WATER_INJECTION is approximately 1,74E+5 [m³] of water. Test-case WATER_INJECTION consist of (10 x 10 x 4) 400 grid blocks.. The Cartesian grid is composed of blocks with the size 30,40 [m] x 30,40 [m] x 2,05 [m]. This leads to a total block volume of 1.894, 53 [m³]. All blocks are set to a permeability of 75 [mD].

To construct this reservoir more sophisticatedly, WATER_INJECTION offers an important feature. The reservoir is divided into four vertical layers: While the injector "I1" releases the fluid into the lower bottom layers, the producer "P1" exploits the water from the upper layers. A schematic illustration of both flow-features of WATER_INJECTION can be seen in Figure 4-29.
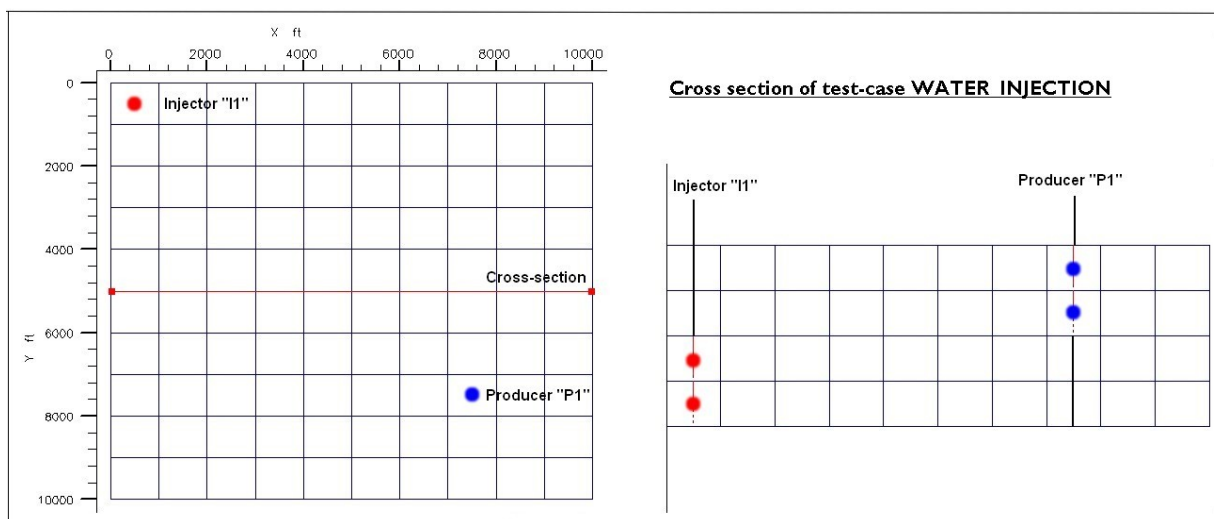

Figure 4-29:   Production scenario of test-case WATER_INJECTION

The configuration in Figure 4-30 forces the fluid not only to flow along the x/y-axis, but also in vertical direction and pressure loss between these two wells can be recorded.

In the next step production conditions for the test-case are set up. Important properties of the injection-production process are listed in Table 4-14:

	Variables	Description	Values	Units
general properties:	TVD	reference depth	2059	[m]
	t	simulated production time	10	[years]
	Δt	time interval of simulation steps	3	[days]
	Δt_{wr}	file writing interval	3	[days]
	K(z)	grid blocks in z direction	4	[blocks]
	I(x)	grid blocks in x direction	10	[blocks]
	J(y)	grid blocks in y direction	10	[blocks]
	$\sum$ grids	total sum of blocks	400	[blocks]
transport properties:	μ	average viscosity	0,96	[m²/s]
	p_{init}	pressure @ reference depth	2,67E+02	[bar]
rock properties:	ρ	fluid density	1000	[kg/m³]
	Φ	rock porosity	23	[%]
well properties:	$\sum$ well	total number of wells	2	
	r_w	well radius	0,155448	[m]

Table 4-14:   Input parameter for WATER_INJECTION

Simulating an injection-production scenario makes more sense, when both wells are rate controlled and the corresponding pressure are measured at both wells. The resulting BHP plot is more convincing than injection-production rates plot. In test-case WATER_INJECTION a specific rate is injected and produced, which differs just slightly: 610 [m³/day] are produced, 600 [m³/day] of the same fluid is injected. As one can see, well P1 is set to a 10 [m³/day] higher production rate. This difference will lead to a slight decline in BHP.

An identical injection and production rate applied on a closed reservoir will lead to pressure equilibrium during simulation, for this reason a more challenging scenario was creating by this small production rate difference.

In Table 4-15 the memory required for the calculation and the simulation time for both, ECLIPSE and OpenFOAM are compared.

Comparison of simulation time and required memory

Processor: *Intel Core2 Duo CPU P8400 @ 2.26GHz*
System: *32Bit operating system*

WATER INJECTION

	ECLIPSE_300	PRSFoam
Wall clock time: [s]	102	18
Required memory: [MB]	17,11	3,62

Table 4-15: WATER_INJECTION: Comparison of simulation run

As the shoe-box model is the basis for this test-case, PRSFoam needs less recourse, because ECLIPSE uses a compositional solver.

The screenshots in Figure 4-30 have been taken at the end of the simulation period, where similar pressure performance was already established. Results of OpenFOAM are visualized using ParaView, while the results of ECLIPSE are visualized by Schlumbergers Result-Module.
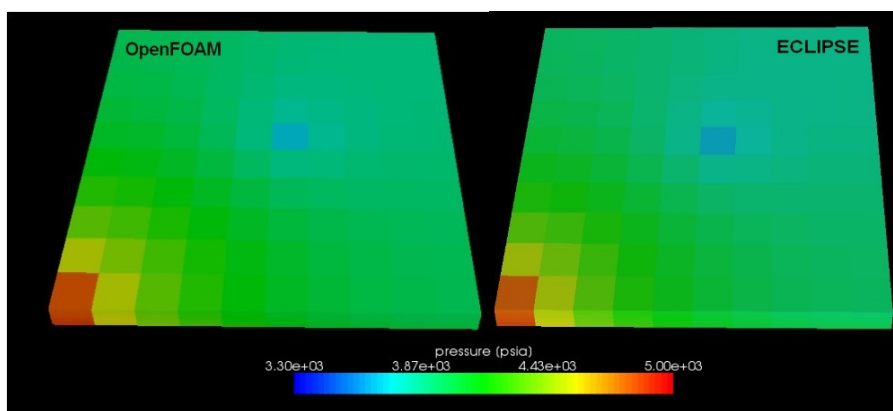
Figure 4-30: WATER_INJECTION: Comparison of ECLIPSE and OpenFOAM

The injector-well in the left corner displaces fluid in the reservoir with a constant rate, causing a pressure increase in this area, while the production well near the center is operated with a higher rate of water and depletes the reservoir. The pressure decrease around the production-block can be seen at the center of Figure 4-30.

According to the simulation of WATER_INJECTION, differences in pressure performance between ECLIPSE and OpenFOAM are listed in Table 4-16.

Summary of WATER_ZONE at constant production/injection rate				
	time-step	well number:	value [psi]	[%]
Result difference between OpenFoam and ECLIPSE	after 1 year	"I1" ECLIPSE - "I1" OpenFOAM	45,99	0,98
		"P1" ECLIPSE - "P1" OpenFOAM	82,35	2,22
	after 2 years	"I1" ECLIPSE - "I1" OpenFOAM	45,45	0,97
		"P1" ECLIPSE - "P1" OpenFOAM	83,74	2,26
	after 5 years	"I1" ECLIPSE - "I1" OpenFOAM	47,41	1,02
		"P1" ECLIPSE - "P1" OpenFOAM	85,60	2,33
	after 10 years	"I1" ECLIPSE - "I1" OpenFOAM	50,74	1,11
		"P1" ECLIPSE - "P1" OpenFOAM	89,05	2,47

Table 4-16: Differences between both simulation tools at constant production-injection rate

As one can see that, both simulation tools, ECLIPSE and OpenFOAM, perform a similar decline in BHP for both wells. Injector well "I1" only differs by 0,98 % - 1,11 % during 10 years of simulation and the production well "P1" range between 2,22 % and 2,47 %, as shown in Table 4-16.

Figure 4-31 represents the resulting graph of this production-injection scenario. All graphs start at 4.000 [psi] and decline or increase corresponding to their positive or negative rate. The predicted BHP's of the OpenFOAM production and injection well are colored blue, while the overall higher performance of ECLIPSE is illustrated by green lines.
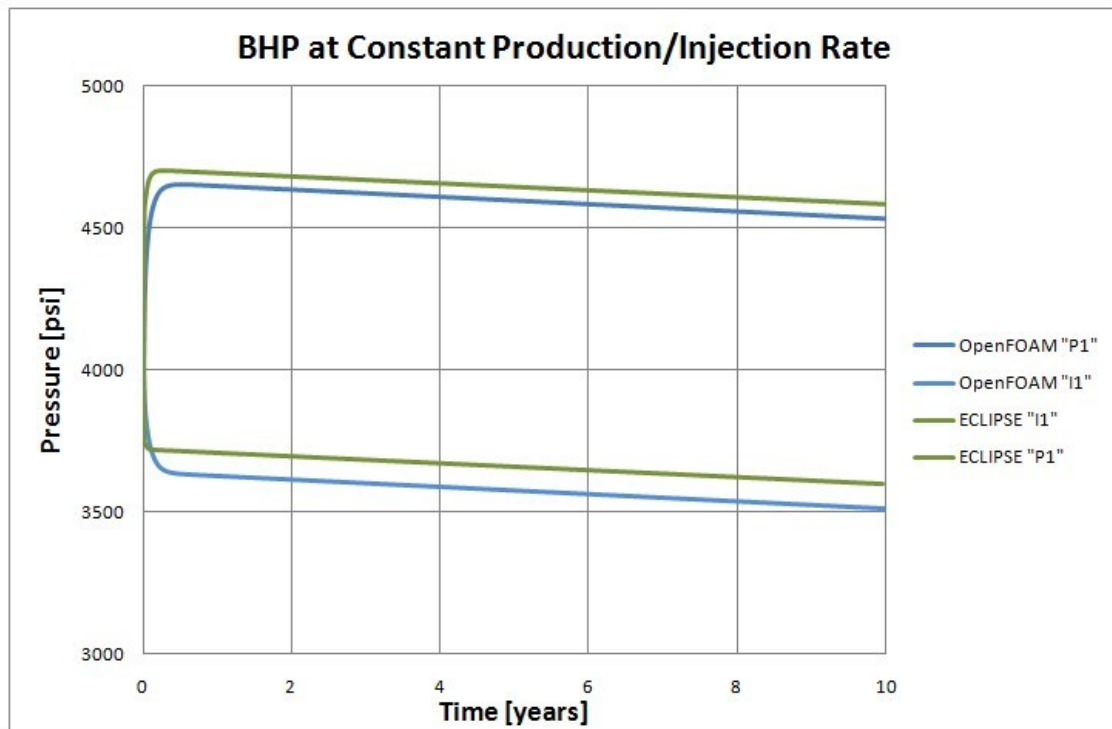
Figure 4-31:   Injection-production performance of WATER_INJECTION

The resulting field performance of WATER_INJECTION is satisfying, since both simulation tools, ECLIPSE as well as OpenFOAM; predict a similar performance of injector "I1" and producer "P1". The pressure difference between injection well "I1" of OpenFOAM and ECLIPSE is approximately 50 [psi], or 1,1 % respectively. The production difference of well "P1" after five years is roughly 86 [psi], or 2,3 %.

Nevertheless, this graph has already convincingly demonstrated that both tools use similar production-injection models and thus result in analogical production and pressure forecasts.

5. Summary and Conclusion

To finally conclude the result of this work the most important plots and tables of all three test-cases are summarized and presented in this chapter.

5.1 Summary

The goal of this thesis was to test the OpenSource software OpenFOAM on its ability to perform reservoir simulation. To do so, a simplified black-oil model solver, PRSFoam was introduced. Its results were compared with Schlumberger's ECLIPSE simulator. For this reason, three test-cases of varying complexity have been designed: TESTCASE_1, TESTCASE_2 and WATER_INJECTION. A comparison of resulting CPU-time and the required disc memory for all three test-cases is listed in Table 5-1.

Comparison of simulation time and required memory

Processor: *Intel Core2 Duo CPU P8400 @ 2.26GHz*
System: *32Bit operating system*

		ECLIPSE	PRSFoam
TESTCASE_1	Wall clock time [s]:	28	2
	Required memory [MB]:	6,75	1,1
TESTCASE_2	Wall clock time [s]:	121	187
	Required memory [MB]:	23,94	35,22
WATER_INJECTION	Wall clock time [s]:	102	18
	Required memory [MB]:	17,11	3,62

Table 5-1: Comparison of CPU-time and required memory of all test-cases

The test-cases were pre-processed with PETREL a commercial software tool of Schlumberger. Resulting data was converted, using *"ECL2FoamGrid"* to translate ECLIPSE cases, written in FORTRAN to OpenFOAM's C++ structure and tested to its integrity.

5.1.1   TESTCASE_1

TESTCASE_1 is also referred to as shoebox-model containing only oil above bubble point pressure within its pores. Structurally the reservoir consists of four high permeable layers isolated on all sides by a closed outer boundary. The results of TESTCASE_1 are of minor validity, since the reservoir is almost symmetrical and distances to walls and wells influence the performance just minimally. Nevertheless, the performance and interference of both simulation tools are satisfying.

Two different simulation scenarios were chosen: production at constant BHP and at constant production rate. The first simulation run consisted of a limited production at constant BHP for all wells. This led to an almost linear decline in production rate. The low internal pressure difference was caused by the homogeneous structure and the symmetrical design of TESTCASE_1. The most meaningful differences of daily production and maximum well differences can be seen in Table 5-1.

Summary of TESTCASE_1 at constant BHP

Differences between OpenFOAM and ECLIPSE	Time-step	Well number:	[STB/day]	[%]
Max.result difference between OpenFoam and ECLIPSE	after 1 year	#2 OpenFOAM - ECLIPSE	180,76	5,04
	after 4 years	#3 OpenFOAM - ECLIPSE	10,57	1,68
Daily production difference between ECLIPSE and OpenFoam:	after 1 year	OpenFOAM - ECLIPSE	469,04	1,85
	after 4 years	OpenFOAM - ECLIPSE	27,63	1,48

Figure 5-1:   Differences of TESTCASE_1 at constant production rate

The second simulation run of TESTCASE_1 consisted of a constant production rate, which was applied to all wells. The BHP decreased rapidly at the beginning and leveled off at a certain pressure rate decline. This rapid decrease was caused by the closed external boundaries, thus isolating the reservoir and limiting the driving forces only to rock compressibility and overburden pressure.

The results shown in Table 5-2 illustrate that the differences between ECLIPSE and OpenFOAM at a constant production rate are less than 0,07 % after one year and just 1,35 % after 4 years.

Summary of TESTCASE_1 at constant production rate				
Differences between OpenFOAM and ECLIPSE	Time-step	Well number:	[psi]	[%]
Max.result difference between OpenFoam and ECLIPSE	after 1 year	#2 ECLIPSE - #2 OpenFOAM	3,22	0,07
	after 4 years	#2 ECLIPSE - #2 OpenFOAM	46,91	1,35

Table 5-2: Comparison between OpenFOAM and ECLIPSE of TESTCASE_1 at constant production rate

5.1.2 TESTCASE_2

Following the positive results of TESTCASE_1 a second test case, named TESTCASE_2 was set up. This consisted of more complex, more realistic geometry. Again, two production scenarios were simulated: a constant production rate and a constant BHP similar for all wells.

Even though TESTCASE_2 offers a more sophisticated basis for reservoir simulation tools the production performance of the PRSFoam solver differs just minimally from the results of the commercial simulator ECLIPSE.

At a constant production rate scenario, all wells of TESTCASE_2 show the similar BHP decline after 5 years of production. OpenFoams pressure results are a little lower than its ECLIPSE counterparts. For example, the maximum difference at well 3 after 20 years is slightly above 4,4 %. OpenFOAM also calculates a shorter transient time for all wells during the first two years. Further distinction between OpenFOAM and ECLIPSE forecasts can be seen in Table 5-3.

Summary of TESTCASE_2 at constant production

Differences between OpenFOAM and ECLIPSE	time-step	well number:	value [psi]	[%]
max. pressure difference between OpenFOAM and ECLIPSE	after 1 year	#1 OpenFOAM - ECLIPSE	59,88	2,81
		#2 OpenFOAM - ECLIPSE	8,09	0,38
		#3 ECLIPSE - OpenFOAM	36,91	1,73
	after 10 years	#1 ECLIPSE - OpenFOAM	5,11	0,26
		#2 ECLIPSE - OpenFOAM	61,00	3,12
		#3 ECLIPSE - OpenFOAM	83,92	4,18
	after 20 years	#1 OpenFOAM - ECLIPSE	0,84	0,04
		#2 OpenFOAM - ECLIPSE	65,67	3,45
		#3 OpenFOAM - ECLIPSE	88,00	4,47

Table 5-3: Differences of TESTCASE_2 at constant production

TESTCASE_2 at constant BHP provides similar differences as results of constant production rate. For example, the cumulative production differs by 1,79 % to 3,24 % between one and 20 years. The difference in daily production varies between 0,91% after the first year and 5,74 % after 20 years of production.

More resulting differences can be seen in Table 5-4.

Summary of TESTCASE_2 at constant BHP				
	time-step	well number:	value [STB/day]	[%]
max. production difference between OpenFoam and ECLIPSE	after 1 year	#1 ECLIPSE - OpenFOAM #2 ECLIPSE - OpenFOAM #3 OpenFOAM - ECLIPSE	70,02 99,97 116,08	3,88 5,50 5,04
	after 10 years	#1 OpenFOAM - ECLIPSE #2 OpenFOAM - ECLIPSE #3 OpenFOAM - ECLIPSE	14,30 65,99 124,43	0,96 4,60 6,60
	after 20 years	#1 OpenFOAM - ECLIPSE #2 OpenFOAM - ECLIPSE #3 OpenFOAM - ECLIPSE	46,63 89,77 119,13	3,39 6,79 6,79
daily production difference between ECLIPSE and OpenFoam:	after 1 year after 10 years after 20 years	ECLIPSE - OpenFOAM OpenFOAM - ECLIPSE OpenFOAM - ECLIPSE	53,91 204,71 255,53	0,91 4,26 5,74
cum. production difference between ECLIPSE and OpenFoam:	after 1 year after 10 years after 20 years	ECLIPSE - OpenFOAM ECLIPSE - OpenFOAM ECLIPSE - OpenFOAM	13681,19 97972,89 378642,87	1,79 1,56 3,24

Table 5-4: Simulation results discrepancy of TESTCASE_2 at constant BHP

Once again, ECLIPSE and OpenFOAM show a similar performance. Further on, well 3 is in both programs an outlier. In contrast to the results of the constant production rate, where all three wells produce similarly at a constant pressure, well number 3 exhibits the ability to produce at higher rates.

Reason being is that well number 3 is set in an area of higher permeability. The resulting field performance can be seen in Figure 5-2.
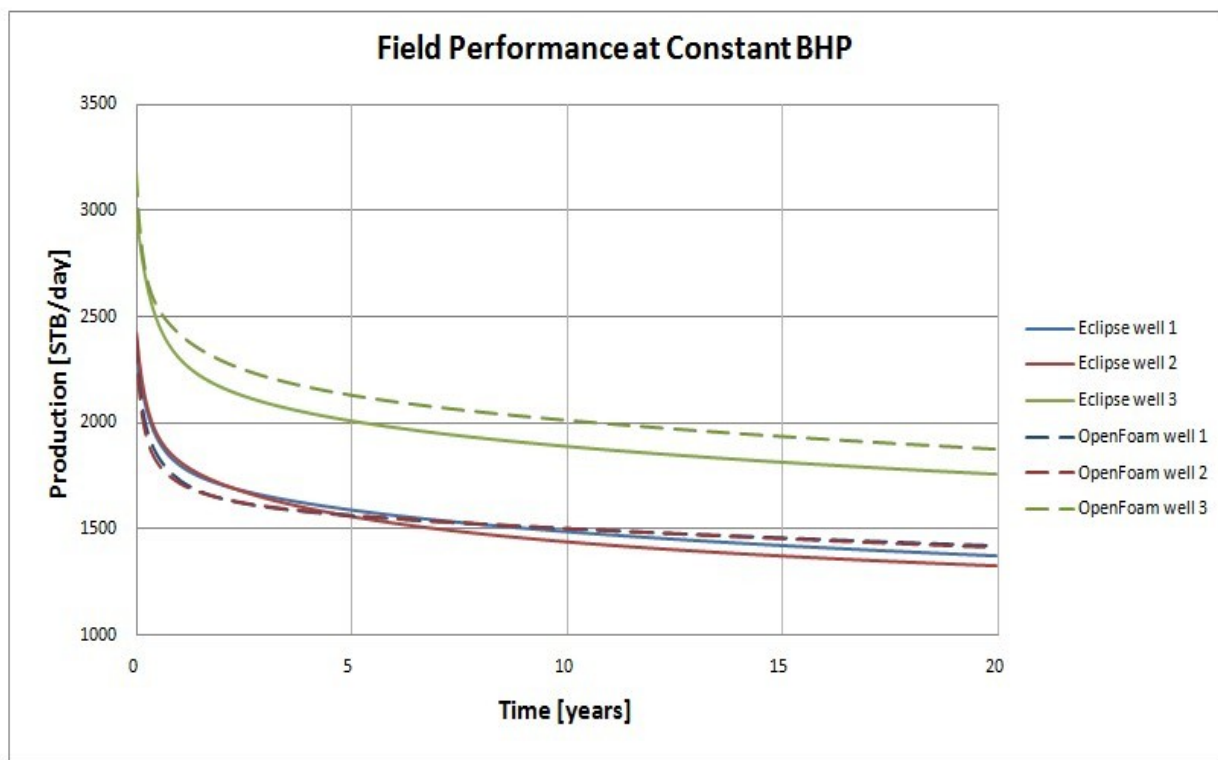
Figure 5-2: TESTCASE_2 complete field performance at constant BHP

It is a very positive finding that both ECLIPSE and OpenFOAM simulate a higher production rate in an inhomogeneous reservoir, where even the permeability of every perforated block is different to its neighbours.

5.1.3   Test-Case WATER_INJECTION

The test-case WATER_INJECTION is also classified as a shoe-box model. The challenge of this study was the 2D flow through the vertical layers and the injection scenario executed by an injector and a production well.

The producer P1 is controlled by a constant production rate, which is slightly higher than the injection rate of well I1.

This setting will guarantee a constant decline in BHP of the reservoir, which can be seen in Figure 5-3.
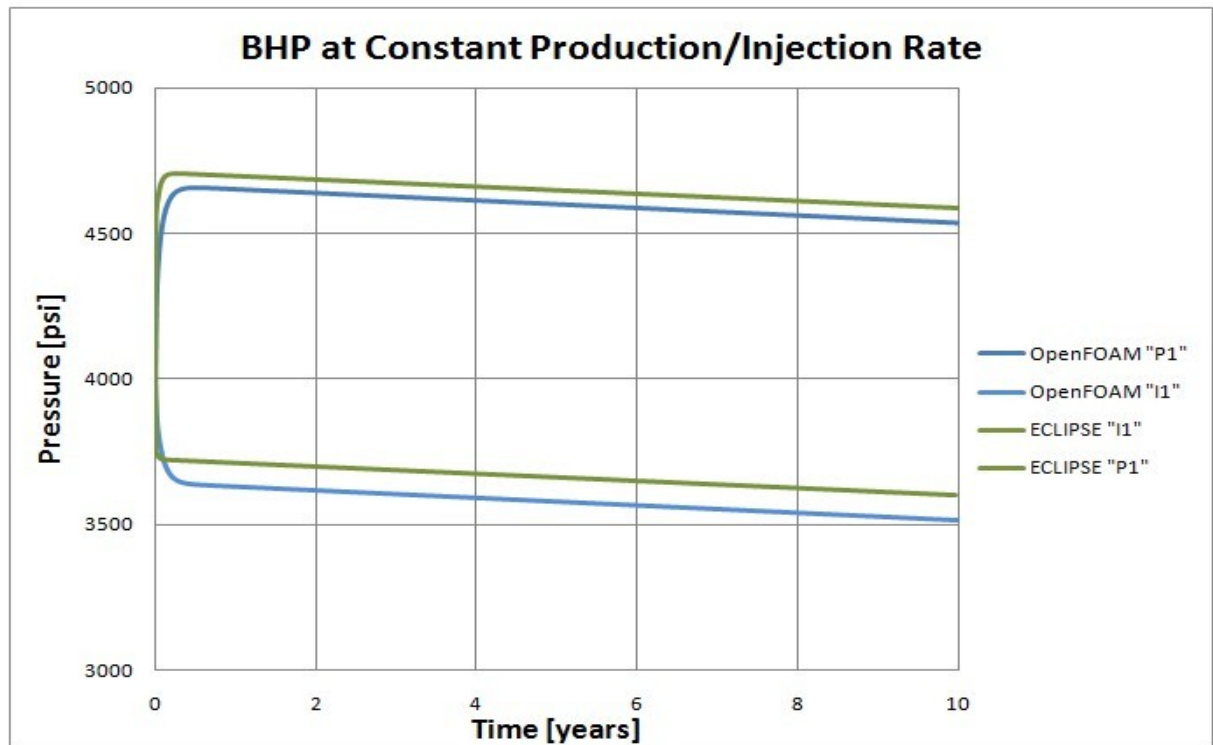
Figure 5-3: Injection / production performance of test case WATER_INJECTION

Production-injection processes can also adequately be simulated using the PRSFoam solver. It has to be considered, that OpenFOAM and ECLIPSE have accepted simplifications and that the WATER_INJECTION test-case constitutes a fictive feasible-model, which does not occur in realistic reservoirs. Nevertheless, the results of the PRSFoam solver for the simulation of displacement process were again satisfactory.

Only minor differences between OpenFOAM and ECLIPSE can be observed in Table 5-5.

Summary of WATER_ZONE at constant production/injection rate				
	time-step	well number:	value [psi]	[%]
Result difference between OpenFoam and ECLIPSE	after 1 year	"I1" ECLIPSE - "I1" OpenFOAM	45,99	0,98
		"P1" ECLIPSE - "P1" OpenFOAM	82,35	2,22
	after 2 years	"I1" ECLIPSE - "I1" OpenFOAM	45,45	0,97
		"P1" ECLIPSE - "P1" OpenFOAM	83,74	2,26
	after 5 years	"I1" ECLIPSE - "I1" OpenFOAM	47,41	1,02
		"P1" ECLIPSE - "P1" OpenFOAM	85,60	2,33
	after 10 years	"I1" ECLIPSE - "I1" OpenFOAM	50,74	1,11
		"P1" ECLIPSE - "P1" OpenFOAM	89,05	2,47

Table 5-5:   Differences between both simulation tools at constant production-injection rate

For example, Injector well "I1" only differs by 0,98 - 1,11 % during 10 years of simulation and the production well "P1" ranges between 2,22 and 2,47 %.

5.2 Conclusion

The results of TESTCASE_1 and test-case WATER_INJECTION are indeed satisfying, as they only differ slightly between OpenFOAM and its commercial counterpart ECLIPSE. TESTCASE_2 exposes the limits of the PRSFoam solver; as it provides a more complex geometry and is highly inhomogeneous, in respect to permeability, porosity and altitude.

From this it can be concluded that OpenFOAM has the potential to introduce students into modern reservoir simulation. Additionally to its capability for reservoir problems, OpenFOAM would offer direct access to the source code this enabling the modification and creation of new solvers and utilities. All the presented advantages of OpenFOAM as reservoir simulation software are emphasized by the fact that it is free, as it is OpenSource. Following this master thesis enhancements in the application range of PRSFoam would be favorable.

Suggested improvements would include:

- Introducing multi-phase phase flow of water, oil and free gas.

- Simulating the rate dependent "skin" in the vicinity of the wellbore. This "near wellbore effect" causes pressure loss by turbulent flow.

- A graphical user interface (GUI) for the future solvers. This would be very helpful for first-time users, as it would assist in, setting up acquired test-cases, reviewing other first-hand examples and helping through the recommended workflow of reservoir simulation.

Considering the comparison between the commercial ECLIPSE simulator and the OpenSource solver PRSFoam, OpenFOAM has a realistic potential of supporting educational reservoir training and E&P projects in the future.

References

[1]   "Reservoir Simulation", by: Zoltan E. Heinemann, Volume 5, Montanuniversity of Leoben, October. 2004

[2]   "Basic Reservoir Simulation", by Heinemann Oil GmbH, February 2007

[3]   "Petroleum Recovery", by Zoltan E. Heinemann, Volume 3, Montan-university of Leoben, 2003

[4]   "Reservoir simulation, Mathematical Techniques in Oil Recovery", Zhangxin Chen, Publisher: SIAM, ISBN: 978-0-898716-40-5, 2007

[5]   "Field Validation of Numerical Simulation Results on the Occurrence and Distribution of Combustible Gas on Onshore Drilling Units", Master Thesis, Klaus Stuhlberger, Chapter: Mathematical Model, Department Mineral Resources and Petroleum Engineering, Montan-university of Leoben, 2006

[6]   "Formulation of a Reservoir Simulation Model", by: Zoltan E. Heinemann, Heinemann Oil GmbH, October 2006

[7]   "Direct methods for sparse matrices", by: Duff, Maurice & Erisman; publisher: Clarendon Pr., ISBN: 0-19-853421-3, 1997

[8]   "Integrated Field Modeling", by: Bamshad Nazarian, ECLIPSE Introduction, Norwegian University of Science and Technology, Department of Petroleum Eng. & Applied Geophysics, December 2002

[9]   "Products of Schlumberger", [www.sbl.com], Products,   October 2008

[10]   "Optimal reservoir control, using nonlinear MPC and ECLIPSE", Patrick Meum, Master Thesis, in Engineering Cybernetics, Norwegian University of Science and Technology, June 2007

[11]   "Tutorial of CFD Basics", [www.opencfd.co.uk], October 2008

[12]   "OpenFOAM, User Guide", The OpenSource CFD Toolbox,
        [http://www.opencfd.co.uk/openfoam/doc/index.html], Version 1.5, July 2008

[13]   "GAMBIT, User Guide", by: Fluent Incorporated, [http://web.njit.edu], February
        2008

[14]   "Petroleum Production Engineering I", by: Gerhard Ruthammer, Montan-university
        of Leoben, 2003

[15]   "ParaView User's Guide", [www.cs.ualberta.ca/~pierreb/Visualization2006], Version
        1.6, 2006

[16]   "Pressure Velocity Coupling", Fluent Incorporated,
        [http://venus.imp.mx/hilario/SuperComputo/Fluent.Inc/manuals], 2007

[17]   "Programmer's Guide", OpenCFD Limited, Version 1.5,
        [http://foam.sourceforge.net/doc/Guides-a4/ProgrammersGuide.pdf], July 2008

[18]   "Engineering fundamentals, Navier-Stokes equation", EFUNDA,
        [http://www.efunda.com/formulae/fluids/navier_stokes.cfm], May 2009

[19]   "FLUENT and GAMBIT Introduction"
        [www.nus.edu.sg/comcen/svu/services/software/fluent.htm], May 2009

[20]   "Lecture Notes of Fluid Flow in Porous Media", by Zoltan E Heinemann, Volume 1,
        Leoben, January 2003

[21]   "ECLIPSE Technical Description", Schlumberger, Version 2004A, 2004

[22]   "ECLIPSE User Guide", Schlumberger, Version 2004A, 2004

[23]   "ECLIPSE Reference Manual", Schlumberger, Version 2004A, 2004

[24]   "Fluid Flow in Porous Media", Volume 1, Zoltan E. Heinemann, Leoben January 2002

[25]   "Petroleum Reservoir Simulation", Aziz K., Settari A., Elsevier Applied Sciences Publishers, London and New York, 1985

[26]   "Nummerische Mathematik für Ingenieure", Jürgen Becker, published byTeuber, 1977

[27]   "Gridding Concept for Third Generation Reservoir Simulator", DR. Dipl.-Ing. Gábor F. Heinemann, Dissertation, Montanuniversity of Leoben, November 2005

[28]   "Petroleum Reservoir Simulation Using Mixed Models" DR. Dipl.-Ing. Leonhard J. Ganzer, Dissitation, Montanuniversity of Leoben, September, 1997

[29]   Product description of REVEAL software, provided by Petroleum Experts Inc., [http://www.petex.com/products/?ssi=8], October 2009

[30]   Homepage of Saudi Aramco, developer of POWERS simulator, [http://www.saudiaramco.com/irj/portal/anonymous], October 2009

[31]   Homepage of Chevron, developer of CHEARS software, [http://www.chevron.com], October 2009

[32]   Product description of Schlumberger'S Petrel seismic simulation software, [http://www.slb.com/content/services/software/geo/petrel/index.asp], October 2009

[33]   "Computational Methods for Multiphase Flow in Porous Media", Zhangxin Chen, Guanren Huan, Yuanle Ma, SIAM, Society for Industrial and Applied Mathematics, 2006

[34]   "Principles of Applied Reservoir Simulation" PD.D. John R. Fanchi, Third Edition, Gulf Professional publisher, 2006

[35]   "Principle of petroleum Reservoir Engineering, Volume 2" Gian Luigi Chierici, Springer Verlag 1995

[36]   "4D Numerical modeling of Petroleum Reservoir Recovery" Margit Munka / József Pápay, Akadémiai Kiadó Budapest, 2001

[37]   "Numerical Heat Transfer and Fluid Flow", Suhas V. Patankar, Hemisphere
       Publishing Corporation, 1980

[38]   "Enhanced Oil Recovery", Dr. Brigitte E. Weinhardt, University of Leoben, 2002

Nomenclature

A	= Cross-section of the porous media	[m²]
B	= Formation volume factor	[ ]
c_R	= Rock compressibility	[1/Pa]
Dp	= Hydraulic diffusity or piezometric conductivity	[m²/s]
Δp_v	= vertical pressure difference	[bar]
g	= Gravity	[m/s²]
h	= Height	[m]
k	= Permeability of the porous media	[m²]
L	= Length of the porous medium in the direction of flow [m]	
Δp	= Pressure difference along the porous medium	[Pa]
p	= Pressure	[Pa]
q	= Production rate	[m³/s]
R_{SO}	= Dissolved gas-oil ratio	[ ]
S	= Saturation	[ ]
S_f	= Cross sectional face	[m²]
t	= Time	[s]
T	= Temperature	[°K]
T	= Transmissibility of the fluid	[m.s]
u	= Fluid velocity	[m/s]
V_T	=Total volume of the sample	[m³]
V_P	= Volume of pore space	[m³]
V_S	= Volume of the solid	[m³]
W	= Molecular weight of the component	[kg/mole]

x	= Distance in x-direction	[m]
y	= Distance in y-direction	[m]
z	= Vertical z-direction; depth	[m]
ϕ	= Porosity	[ ]
ϕ^0	= Porosity at the reference pressure	[ ]
λ	= Phase mobility	[m.s / kg]
Ψ	= Potential function	[Pa]
ρ	= Density	[kg/m³]
μ	= Viscosity of the flowing fluid	[Pa.s]
γ	= Fluid gravity	[Pa/m]
α	= Phases: water, oil or gas	[ ]
BHP	= Bottom hole pressure	[Pa]
CFD	= Computational fluid dynamics	
FVF	= Formation volume factor	
GUI	= Graphical user interface	
STB	= Standard tank barrel	

Appendix A: Log-Files of ECLIPSE and OpenFOAM simulation

Log File of the ECLIPSE Simulation:

```
    1 READING RUNSPEC
    2 READING TITLE
    3 READING START
    4 READING METRIC
    5 READING UNIFOUT
    6 READING OIL
    7 READING MONITOR
    8 READING RSSPEC
    9 READING DIMENS
   10 READING EQLDIMS
   11 READING REGDIMS
   12 READING TABDIMS
   13 READING WELLDIMS
   14 READING GRID
eclipse for use by eclipse  Locked  - Expiry Date 8-sep-2001


   LIST OF ECLIPSE 100 SPECIAL OPTIONS
   ===================================

POLYMER FLOOD          -    -    -    -    -    -    -    -    -    AVAILABLE
NETWORKS     -    -    -    -    -    -    -    -    -    AVAILABLE
LOCAL GRID REFINEMENT/COARSENING    -    -    -    -    -    AVAILABLE
FLUX BOUNDARY OPTION     -    -    -    -    -    -    -    AVAILABLE
SOLVENT FLOOD MODEL    -    -    -    -    -    -    -    -    AVAILABLE
GAS FIELD OPERATIONS MODEL -    -    -    -    -    -    -    AVAILABLE
WELLBORE FRICTION OPTION   -    -    -    -    -    -    -    AVAILABLE
GI-MODEL     -    -    -    -    -    -    -    -    -    AVAILABLE
SURFACTANT FLOOD -    -    -    -    -    -    -    -    -    AVAILABLE
GAS LIFT OPTIMISATION -    -    -    -    -    -    -    -    AVAILABLE
PARALLEL OPTIONS -    -    -    -    -    -    -    -    -    AVAILABLE
ENVIRONMENTAL TRACERS -    -    -    -    -    -    -    -    AVAILABLE
COAL BED METHANE OPTION  -    -    -    -    -    -    -    AVAILABLE
MULTI-SEGMENT WELL OPTION  -    -    -    -    -    -    -    AVAILABLE
RESERVOIR COUPLING    -    -    -    -    -    -    -    -    AVAILABLE
FOAM MODEL   -    -    -    -    -    -    -    -    -    AVAILABLE
GAS QUALITY CONTROL OPTION -    -    -    -    -    -    -    AVAILABLE
SIMOPT/HUTS GRADIENTS -    -    -    -    -    -    -    -    AVAILABLE


   THE PRESENT PROGRAM/PASSWORD COMBINATION EXPIRES ON  8/SEP/2001


   16 READING GRIDFILE
   17 READING INIT
   18 READING INCLUDE E:\Programme\eclipse\2001a_2\model_feb09\model_ET_
   19 READING NOECHO
          END OF INCLUDE FILE
   20 READING INCLUDE E:\Programme\eclipse\2001a_2\model_feb09\model_ET_
   21 READING MAPAXES
   22 READING GRIDUNIT
   23 READING COORDSYS
   24 READING MAPUNITS
   25 READING COORD
   26 READING ZCORN
          END OF INCLUDE FILE
   27 READING INCLUDE E:\Programme\eclipse\2001a_2\model_feb09\model_ET_
   28 READING ACTNUM
   29 READING PERMX
   30 READING PERMY
   31 READING PERMZ
   32 READING PORO
   33 READING NTG
          END OF INCLUDE FILE
   34 READING INCLUDE E:\Programme\eclipse\2001a_2\model_feb09\model_ET_
   35 READING PINCH
          END OF INCLUDE FILE
   36 READING PROPS

@--MESSAGE  AT TIME        0.0   DAYS   ( 1-JAN-2008):
@          NEITHER OLDTRAN,OLDTRANR NOR NEWTRAN SPECIFIED
@          TRANSMISSIBILITIES TO BE CALCULATED
@          USING  NEWTRAN
```

```
@--COMMENT  AT TIME        0.0   DAYS    ( 1-JAN-2008):
@           NO NON-NEIGHBOUR CONNECTIONS FOUND

@--MESSAGE  AT TIME        0.0   DAYS    ( 1-JAN-2008):
@           NUMBER OF ACTIVE CELLS IS    36400

@--MESSAGE  AT TIME        0.0   DAYS    ( 1-JAN-2008):
@           PROBLEM REQUIRES     23.025 MEGABYTES
@              663 ( BYTES PER ACTIVE CELL )

@--MESSAGE  AT TIME        0.0   DAYS    ( 1-JAN-2008):
@           40402 CHARACTER VARIABLES USED
   37 READING INCLUDE E:\Programme\eclipse\2001a_2\model_feb09\model_ET_
   38 READING ECHO
   39 READING PVDO
   40 READING DENSITY
   41 READING ROCK
           END OF INCLUDE FILE
   42 READING INCLUDE E:\Programme\eclipse\2001a_2\model_feb09\model_ET_
           END OF INCLUDE FILE
   43 READING SOLUTION
   44 READING INCLUDE E:\Programme\eclipse\2001a_2\model_feb09\model_ET_
   45 READING EQUIL
   46 READING ECHO
   47 READING RPTRST
           END OF INCLUDE FILE
   48 READING SUMMARY
   49 READING INCLUDE E:\Programme\eclipse\2001a_2\model_feb09\model_ET_
   50 READING WOPR
   51 READING WBHP
   52 READING FOPR
   53 READING FPR
           END OF INCLUDE FILE
   54 READING SCHEDULE
   55 READING INCLUDE E:\Programme\eclipse\2001a_2\model_feb09\model_ET_
   56 READING ECHO
   57 READING NOECHO
   58 READING TUNING
   59 READING ECHO
   60 READING RPTRST
   61 READING NOECHO
   62 READING WELSPECS
   63 READING WELSPECS
   64 READING WELSPECS
   65 READING COMPDAT
   66 READING COMPDAT
   67 READING COMPDAT
   68 READING WCONPROD

@--WARNING  AT TIME        0.0   DAYS    ( 1-JAN-2008):
@           THE BOTTOM HOLE PRESSURE LIMIT FOR WELL IFR_01
@           HAS BEEN DEFAULTED.  THE DEFAULT VALUE IS
@              1.0   BARSA
   69 READING WCONPROD

@--WARNING  AT TIME        0.0   DAYS    ( 1-JAN-2008):
@           THE BOTTOM HOLE PRESSURE LIMIT FOR WELL IFR_02
@           HAS BEEN DEFAULTED.  THE DEFAULT VALUE IS
@              1.0   BARSA
   70 READING WCONPROD

@--WARNING  AT TIME        0.0   DAYS    ( 1-JAN-2008):
@           THE BOTTOM HOLE PRESSURE LIMIT FOR WELL IFR_03
@           HAS BEEN DEFAULTED.  THE DEFAULT VALUE IS
@              1.0   BARSA
   71 READING DATES

@--MESSAGE  AT TIME        0.0   DAYS    ( 1-JAN-2008):
@           RESTART FILE WRITTEN   REPORT     0
STEP    1 TIME=    3.10  DAYS ( +3.1  DAYS INIT  1 ITS) (4-JAN-2008)

 PAV=   206.3  BARSA  WCT= 0.00 GOR= 0.00000   SM3/SM3 WGR= 0.00000   SM3/SM3
```

Log File of the OpenFOAM Simulation:

```
/*--------------------------------*- C++ -*----------------------------------*\
| =========                 |                                                 |
|                           |                                                 |
| \\        /   F ield      | OpenFOAM: The Open Source CFD Toolbox           |
|                           |                                                 |
|  \\     /    O peration   | Version:  1.4.1                                 |
|                           |                                                 |
|   \\   /     A nd         | Web:      http://www.openfoam.org               |
|                           |                                                 |
|    \\/       M anipulation |                                                |
|                           |                                                 |
\*---------------------------------------------------------------------------*/
Exec  : PRSFoam . onePhaseModel1
Date  : Sep 08 2009
Time  : 08:39:24
Host  : mint
PID   : 4273
Root  : /home/stephan/Desktop
Case  : onePhaseModel1
Nprocs : 1

Create time
Create mesh for time = 0
Reading transport  properties
Reading field p
creating permeability k
Reading PERMX
Reading PERMY
Reading PERMZ
Reading porosity fi
Reading viscosity  muO
Reading Poroelastic  storage coefficient cP
Reading field I_INDEX
Reading field J_INDEX
Reading field K_INDEX
Reading field I_INDEX
Reading field J_INDEX
Reading field K_INDEX
Reading field DEPTH

Reading well description  dictionary
Creating well from well description  file
reading wells :

one well read  : 2(1479 2079)   qsf: qsf [0 3 -1 0 0 0 0] 0.00736052    pwf: pwf [1 -1 -2 0 0 0 0] 0
well_1: 2{0}
well well_1 is rate control  with qsf = 0.00791256pwf  is set to default: 0
end of wellCellList::newWell(...)

one well read  : 2(1484 2084)   qsf: qsf [0 3 -1 0 0 0 0] 0.00791256    pwf: pwf [1 -1 -2 0 0 0 0] 0
well_2: 2(1.42494e-313 8.69594e-311)
well well_2 is rate control  with qsf = 0.00754454pwf  is set to default: 0
end of wellCellList::newWell(...)
one well read  : 2(1489 2089)   qsf: qsf [0 3 -1 0 0 0 0] 0.00754454   pwf: pwf [1 -1 -2 0 0 0 0] 0
```

Debug: wellCellList::VCell_: 6(623818 623818 623821 623821 623816 623816)
creating wellIndex Field

wells.PICell_: 6(-2.17545e-09 -2.17545e-09 -2.17545e-09 -2.17545e-09 -2.17545e-09 -2.17545e-09)
wells.qCell_: 6(0.00368026 0.00368026 0.00395628 0.00395628 0.00377227 0.00377227)
wells.VCell_: 6(623818 623818 623821 623821 623816 623816)
wells.DxCell_: 6(115.252 115.252 115.251 115.251 115.251 115.251)
wells.DyCell_: 6(107.214 107.214 107.215 107.215 107.214 107.214)
wells.DzCell_: 6(50 50 50 50 50 50)
wells.rEqCell_: 6(22.0374 22.0374 22.0374 22.0374 22.0374 22.0374)
wells.addressing_: 6(1479 2079 1484 2084 1489 2089)

Reading mechanical properties
Normalising E : E/rho
Calculating Lame's coefficients
Plane Strain
mu = 48970.6 Pa/rho
lambda = 73456 Pa/rho
threeK = 318309 Pa/rho
Reading thermal properties

Starting initialization :
wellCellList::initializeGraphData() outputsize=19
creating fields for generating graphs of well data
iIndex_[1479]=10
kIndex_[1479]=2
iIndex_[2079]=10
kIndex_[2079]=1
iIndex_[1484]=15
kIndex_[1484]=2
iIndex_[2084]=15
kIndex_[2084]=1
iIndex_[1489]=20
kIndex_[1489]=2
iIndex_[2089]=20
kIndex_[2089]=1
end of initializeGraphData()
end of void wellCellList::initializeGraphData()

Starting time loop :

Time = 3.65 day
DICPCG: Solving for p, Initial residual = 0.500942, Final residual = 0.0165163, No Iterations 2
ExecutionTime= 0.09 s ClockTime= 0 s